A statistical test on the local effects of spatially structured variance

Spatial variance is an important characteristic of spatial random variables. It describes local deviations from average global conditions and is thus a proxy for spatial heterogeneity. Investigating instability in spatial variance is a useful way of detecting spatial boundaries, analysing the internal structure of spatial clusters and revealing simultaneously acting geographic phenomena. Recently, a corresponding test statistic called 'Local Spatial Heteroscedasticity' (LOSH) has been proposed. This test allows locally heterogeneous regions to be mapped and investigated by comparing them with the global average mean deviation in a dataset. While this test is useful in stationary conditions, its value is limited in a global heterogeneous state. There is a risk that local structures might be overlooked and wrong inferences drawn. In this article, we introduce a test that takes account of global spatial heterogeneity in assessing local spatial effects. The proposed measure, which we call 'Local Spatial Dispersion' (LSD), adapts LOSH to local conditions by omitting global information beyond the range of the local neighbourhood and by keeping the related inferential procedure at a local level. Thereby, the local neighbourhoods might be small and cause small-sample issues. In the view of this, we recommend an empirical Bayesian technique to increase the data that is available for resampling by employing empirical prior knowledge. The usefulness of this approach is demonstrated by applying it to a LiDAR-derived dataset with height differences and by making a comparison with LOSH. Our results show that LSD is uncorrelated with non-spatial variance as well as local spatial autocorrelation. It thus discloses patterns that would be missed by LOSH or indicators of spatial autocorrelation. Furthermore, the empirical outcomes suggest that interpreting LOSH and LSD together, is of greater value than interpreting each of the measures individually. In the given example, local interactions can be statistically detected between variance and spatial patterns in the presence of global structuring, and thus reveal details that might otherwise be overlooked.

Keywords: spatial analysis; spatial heterogeneity; spatial hypothesis testing; spatial non-stationarity

1. Introduction

Geographic instability in statistical parameters (called 'spatial heterogeneity', s. Dutilleul and Legendre 1993) has long been of scientific interest. Alexander von Humboldt noted a distinctive geographic patchiness in the 19th century (Sparrow 1999), and Darwin´s theory of evolution was largely driven by his recognition of a geographic distribution of phenotypic variants (Jacquez 2010). Currently, scholars from empirical research subjects such as ecology, epidemiology or sociology, leverage knowledge out of spatial heterogeneity to either detect and specify zones of transition (e.g., transitions from terrestrial to aquatic habitats (Turner 1989)), to link local to global processes (Berkes *et al.* 2006), or to acquire a better understanding of the ecological complexity of urban areas (Cadenasso *et al.* 2007).

Despite its useful properties, spatial heterogeneity plays a relatively minor role in spatial analysis techniques, which are mostly designed for clustering. Measures of spatial autocorrelation and hot spot techniques are prevalent, and these are used to assess associations within spatial random variables (Getis 2010). In contrast, spatial heterogeneity is often deemed to be a technical nuisance and seldom regarded as a source of valuable information. It either requires a methodological approach (Anselin 1988, Páez and Scott 2004, Graif and Sampson 2009), or is considered to be reminiscent of large-scale structures that influence local patterns (e.g., Ord and Getis 2001). Spatial heterogeneity indeed undermines the stationarity assumptions that form the basis of many spatial techniques (Gaetan and Guyon 2010, p. 166 ff.). Thus, regarding it from the standpoint of a nuisance is partly justified.

Nonetheless, spatial heterogeneity often contains useful information. A good illustration of this is the recent investigation of the domiciles of newly arrived migrants from rural areas to Accra, Ghana (Getis 2015). The use of spatial variance as a proxy for spatial heterogeneity allows transitional zones to be detected between the underdeveloped and wealthy districts of the city. Incoming migrants from rural parts of Ghana first settle in these transitional areas after they first arrive in the city. This recent example shows that spatial heterogeneity can supply important information to investigations of complex geographic situations, and lead to useful conclusions of both a theoretical and practical value.

Spatial heterogeneity is also important for the analysis of intrinsically heterogeneous and novel data sources. Social media data, for instance, are sometimes called the 'big noise' (Lovelace *et al.* 2016), because they are characterised by unstable 'wild variance' (Jiang 2015). The latter is characterised by an interaction between spatial patterns and variance, which influences analysis results. Westerholt et al. (2015, 2016) recently found that spatial heterogeneity causes Type I errors, topological outliers and some further problems that are relevant to the spatial analysis of Twitter data. As a result, many researchers are now investigating social media data in an attempt to mitigate its noisy features (e.g., Sengstock et al. 2013, Lovelace et al. 2016, Steiger et al. 2016). The investigation of heterogeneity, however, might provide a clue about the spatial perceptions of people and help to characterise the users' everyday behaviours more accurately. Similar arguments hold true for the data obtained from multi-temporal analysis. The differences between multi-temporal data acquired by 'Light Detection and Ranging' (LiDAR) (Fang and Huang 2004, Tian *et al.* 2014), for example, are a means of detecting heterogeneous changes in surface phenomena. When investigating the LiDAR recordings of landslides (Jaboyedoff *et al.* 2012), it was found that spatial heterogeneity can provide a wealth of information about significant morphological features like differently shaped earth deposits (Hungr *et al.* 2014). These two rather different examples demonstrate the potential value of investigating spatial heterogeneity in a number of application scenarios.

Recently, a statistical measure of spatial variance called 'Local Spatial Heteroscedasticity' (LOSH; Ord and Getis 2012) was put forward as a means of investigating spatial heterogeneity. LOSH assesses the effects of spatial patterns on the variance of an attribute. It identifies regions in which the *local* spatial variance deviates

from the *global* average variability. The measure thus reveals and maps structures of the variance that are at least partially global in nature, whereas the weaker structures that are entirely local remain hidden. The latter only feature prominently in local circumstances but remain undetected by the global reference framework of LOSH.

We set out a technique that extends LOSH by making it a measure for the influence of local spatial patterns on local variance. The test, which we call 'Local Spatial Dispersion' (LSD), makes it possible to detect whether the local geographic arrangement of random variables increases or reduces the variance. This is carried out in an *entirely local* manner and takes no account of global characteristics. In addition, we propose an entirely local bootstrapping approach for drawing inferences. Drawing inferences that are only local, however, entails limited amounts of data from small local neighbourhoods. As a means of circumventing the problem of small-size samples within these local subsets, (which particularly arises when adjusting small analytical scales), the inference technique includes an empirical Bayesian prediction of additional synthetic local data. The usefulness of the proposed technique can be demonstrated by applying it to a high-resolution 3D change detection dataset. The data is derived from a long-term 'automatic terrestrial laser scanning station' (ATLS) that covers a slow-moving landslide in Gresten, Austria and provides a useful scenario because it contains both a distinct global structure and additional local patterns.

The paper starts with a detailed review of spatial heterogeneity and spatial heteroscedasticity, and includes a brief discussion of related statistical methodologies (Section 2). Following this outline, LOSH and our proposed measure are introduced (Sections 3 and 4). Then, there is a Bayesian prediction of residuals as well as the bootstrap method for developing predictive models (Section 5), before the empirical results are discussed (Session 6) and the final conclusions are drawn (Section 7).

2. Related work: Spatial heterogeneity and spatial heteroscedasticity

Spatial heterogeneity refers to non-uniformity and instability in geographic random variables (Dutilleul and Legendre 1993). Their corresponding zones 'where variables change rapidly' (Jacquez 2010, p. 210) are of scientific and practical interest. They can i) represent regions of habitat use and ecological interactions (Fagan *et al.* 1999, Lohrer *et al.* 2013), ii) assist in testing ethno-racial diversity (Abascal and Baldassarri 2015, Legewie and Schaeffer 2016), or iii) touch on the question of disease transmission (Grillet *et al.* 2010, Perkins *et al.* 2013). Spatial heterogeneity is also important for urban studies. Metaphorically speaking, just as prices in economic markets do not 'glide' but often 'leap' (Mandelbrot and Hudson 2004), urban regions tend to be heterogeneous and disruptive in nature (Cadenasso *et al.* 2007). Analysing heterogeneity is thus of crucial importance for understanding urban social processes, while an analysis of boundaries can assist in distinguishing subpopulations. Furthermore, spatial heterogeneity provides guidance in testing assumptions and theories about the relationships between variables (Jacquez 2010), as well as assisting in data aggregation and dynamic modelling (Anselin 1990).

Different structural types of spatial heterogeneity are distinguishable. These are characterised by their causal origins, maintenance mechanisms, spatial structures, and functional and temporal dynamics (Strayer *et al.* 2003). Other more technical distinguishing factors include the types of investigated variables (Wagner and Fortin 2005), the underlying spatial indexes (spatially discrete vs. continuous; Anselin 2010) and even the methodological perspectives that researchers adopt (dynamic modelling vs. hypothesis testing; Fagan et al. 2003). In structural terms, heterogeneous zones sometimes condense to thin and crisp boundaries, while they can also appear fuzzy (Jacquez *et al.* 2000).

For functional purposes, heterogeneous zones can act as semipermeable filters or conduits and as devices from which spatial processes either originate or where they are impeded (Forman 1995). Steep gradients or threshold conditions, at which variable states change suddenly, can also be found in heterogeneous areas (Fagan *et al.* 2003). These characteristics allow the spatial heterogeneity to exert a short or long-range influence on dynamic processes (Fagan *et al.* 2003). Sometimes these influences get strengthened by the interrelations between the effects mentioned earlier, especially by the interplay between the structural and functional characteristics (Laurance *et al.* 2001). Hence, the various features, together with the number of functional influences, show the importance of investigating spatially heterogeneous zones.

Techniques to detect heterogeneous zones (especially crisp boundaries), first appeared in image processing. Some corresponding methods have been designed for segmenting synthetic images, although they are not capable of depicting dynamic real-world systems in their entirety (Goovaerts 2010). A range of more suitable methods has thus evolved, including techniques based on moving split-windows (Fortin 1994, 1999, Kent et al. 1997, 2006), first-order derivatives (‘Wombling’, Womble 1951, Barbujani et al. 1989, Gelfand and Banerjee 2015), second-order derivatives (Fagan *et al.* 2003, Lillesand *et al.* 2015), spatially constrained clustering (Jacquez *et al.* 2000, Patil *et al.* 2006, Bravo and Weber 2011), fuzzy set modelling (Arnot and Fisher 2007, Fisher and Robinson 2014), wavelets (Csillag and Sándor 2002, Keitt and Urban 2005, Ye *et al.* 2015) and several further parametric as well as non-parametric techniques (Jacquez *et al.* 2008, Wang *et al.* 2016). Another closely related research field is concerned with integrating spatial heterogeneity with quantitative models. The respective approaches include the following: hierarchical and Bayesian concepts (Lee and Mitchell 2012, Anderson *et al.* 2014, Hanson *et al.* 2015), geostatistical techniques (Garrigues *et al.* 2006, Goovaerts 2008, Hu *et al.* 2015), extensions to global spatial regression methods (Anselin 2001), and the local geographically-weighted regression approach (Fotheringham *et al.* 1996, 2002, Brunsdon *et al.* 1998).

In statistics, heterogeneity either refers to single parameters (e.g., mean or variance) or to complete distributions (Kolasa and Rollo 1991, Dutilleul and Legendre 1993). Spatial heterogeneity can be decomposed into a deterministic, random and chaotic parts (Dutilleul 2011). The deterministic part reflects the varying average component (‘large-scale trend’), while the latter two together reflect variations caused by variance instability (‘unstable mean deviations’) and spatial autocorrelation (‘variation through interaction’). It is necessary to differentiate between heterogeneities

in different parameters and also between the three parts outlined above, to achieve a thorough understanding of the behaviour of random variables and related phenomena.

In spatial analysis, varying means are analysed by hot spot techniques like the G and the O-statistic (Getis and Ord 1992, Ord and Getis 1995, 2001). By analogy, variations caused by autocorrelation are analysed through local measures of spatial autocorrelation like the 'Local Indicators of Spatial Association' (LISA, Anselin 1995). While these cases have been widely investigated, there has been comparatively little research on variability in the variance (called 'spatial heteroscedasticity'; Dutilleul and Legendre 1993). Roughly speaking, spatial heteroscedasticity refers to 'wild variance' (Jiang 2015). Ord and Getis (2012) recently put forward a local measure called 'Local Spatial Heteroscedasticity' (LOSH), which assesses spatial structure in variance and is akin to a spatial χ^2 test. Xu et al. (2014) investigated the distributional properties of LOSH and found that the χ^2 approximation proposed by Ord and Getis (2012) is not always suitable, and that a Monte Carlo bootstrap should be used instead.

LOSH is ideally suited to detecting boundary-like sub-regions lying *between* homogeneous regimes. However, it cannot describe in detail how local spatial arrangements of random variables in place affect the heterogeneity *within* the individual sub-regions. This is where our study is able to make a contribution to the field because it supplements LOSH by conducting a test involving the local spatial microstructure of the variance of georeferenced random variables.

3. Local spatial heteroscedasticity (LOSH)

The LOSH measure (Ord and Getis 2012) calculates local deviations from the global average variance. It is derived from the hot spot technique called 'G-statistic' (Getis and Ord 1992, Ord and Getis 1995) and allows boundaries and hot spots of high variability to be detected. LOSH tests the following hypotheses:

$\boldsymbol{H_0^{LOSH}}$: *The variance in a region does not deviate markedly from its global average.*
$\boldsymbol{H_1^{LOSH}}$: *The variance in a region deviates from overall variance homogeneity.*

LOSH proceeds as follows: In the first stage, residuals that describe the difference between an attribute value and its local spatially weighted mean value are estimated. In each location, the spatially weighted averages of these residuals are then compared with their global counterpart. The latter is estimated with data from all locations by randomising the spatial pattern at the same time. The calculated ratio of these two averages then forms a test statistic from which inferences can be drawn. Let X be a set of n real-valued random variables X_i referenced in an index set $\mathcal{N} = \{1, \dots, n\}$ that indicates discrete spatial units. By analogy, let $\mathcal{N}_i = \{ j \in \mathcal{N} \mid \exists i \in \mathcal{N} : w_{ij} \neq 0 \}$ be the local neighbourhood of spatial unit i that can be defined by suitable spatial weights, whereby the choice of the latter depends on the application scenario. These weights, which are given by W, a symmetric matrix of elements w_{ij} that map pairs of spatial units to positive real weights, are a mathematical representation of the geographical layout of the investigated region (Dray 2011). The weight matrix thereby limits the

entire geographic layout to those geographic features that are relevant to a particular phenomenon under study. These weights can be of an arbitrary shape (s. Bavaud 2014 for an overview) and no specific form is required for the remainder. LOSH (H_i is the notation for LOSH chosen by (Ord and Getis 2012)) then reads as

$$H_i = \frac{\sum_{j\in\mathcal{N}} w_{ij}|e_j|^a}{h_1 \sum_{j\in\mathcal{N}} w_{ij}}, \quad e_j = x_j - \bar{x}_j, \quad \bar{x}_j = \frac{\sum_{k\in\mathcal{N}_j} w_{jk}x_k}{\sum_{k\in\mathcal{N}_j} w_{jk}} \quad \text{and} \quad h_1 = \frac{\sum_{j\in\mathcal{N}}|e_j|^a}{n}, \quad (1)$$

where e_j is a residual about a local spatially weighted mean $\bar{x}_j$ and h_1 is the overall average residual estimated from all the spatial units in the region. Note that $\mathcal{N}_j$ is the neighbourhood around unit j, that is defined analogously to $\mathcal{N}_i$. Exponent a allows different types of mean deviations to be investigated. For the remainder of this paper, we adjust $a = 2$ and confine the discussion to a measure of variance.

An inference about LOSH assumes random permutations of the residuals. When an average residual h_1 is employed, it thus makes clear that LOSH assumes weak stationarity in the null hypothesis. The successful detection of a local pattern thus depends on the global reasonability of h_1. Through a random permutation of the residuals, the statistic obtains an expected value of $E[H_i] = 1$ and has a variance of

$$V_i[H_i] = \frac{1}{n-1}\left(\frac{1}{h_1 \sum_{j\in\mathcal{N}} w_{ij}}\right)^2 \left[\frac{1}{n}\left(\sum_{j\in\mathcal{N}}|e_j|^{2a} - \left[\sum_{j\in\mathcal{N}}|e_j|^a\right]^2\right)\right]\left(n\sum_{j\in\mathcal{N}} w_{ij}^2 - \left[\sum_{j\in\mathcal{N}} w_{ij}\right]^2\right). \quad (2)$$

Ord and Getis (2012) propose an adjusted χ^2 approximation to the null distribution as a parametric solution to statistical inference. The χ^2 distribution stems from the design of the statistic as a spatialised variant of the classic χ^2 test for testing deviations from a hypothesised variance. This is seen by writing out the individual terms of the sum from Equation (1):

$$H_i = \frac{w_{i1}}{\sum_{j\in\mathcal{N}} w_{ij}} \frac{|e_1|^2}{h_1} + \cdots + \frac{w_{ij}}{\sum_{j\in\mathcal{N}} w_{ij}} \frac{|e_j|^2}{h_1} + \cdots + \frac{w_{in}}{\sum_{j\in\mathcal{N}} w_{ij}} \frac{|e_n|^2}{h_1}. \quad (3)$$

Variable h_1 is the hypothesised variance and the summands are (spatially weighted) squared standardised residuals. Under normality constraints, these are χ^2 with one degree of freedom. Their sum is then χ^2 with additive degrees of freedom (Cochran 1934). On the basis of the findings from Box (1953), Ord and Getis (2012) adjust LOSH to take better account of non-normality by including the empirical variance V_i. This matches the χ^2 approximation to the observed outcomes and controls the shape of the reference distribution. The skew and the excess kurtosis of the reference distribution are given by $\gamma_1 = 2\sqrt{V_i}$ and $\gamma_2 = 6V_i$, and the test statistic is $Z_i = 2H_i/V_i$ with $2/V_i$ degrees of freedom. However, Xu et al. (2014) found deviations between empirical distributions obtained from data and the adjusted approximation outlined above. These even occur with normal variables, which is why Xu et al. (2014) suggest adopting a nonparametric bootstrap procedure instead.

4. Local spatial dispersion (LSD)

Instead of comparing local regions with a global average like LOSH, the proposed measure LSD is concerned with the effect of the local spatial pattern on local variances. The underlying assumption is that the way random variables are arranged geographically increases or reduces the variance, or else is unrelated to its characterisation. The measure is only defined in a *local* context and does not take account of global information. The same principle also applies for the related inference procedure, which is conducted locally.

The proposed LSD is useful when a dataset comprises statistically differing sub-regions or when spatially coexisting phenomena are observed. However, global information such as the average residual h_1 is not meaningful in these circumstances. This means the LOSH approach causes problems because it is unrealistic to assume there is weak stationarity in these cases. Instead, the variance patterns might be strongly interacting with the geographic layout locally, although they might not be recognised when a global comparison is made with sub-regions that show a stronger dispersal. Thus LOSH cannot be employed to assess entirely local effects and an entirely local measure of spatial variance, such as LSD, can prove to be useful.

4.1 Hypotheses

The proposed test determines whether the local spatial arrangement of random variables increases or reduces the local variance. The following two hypotheses for LSD are formulated:

$\boldsymbol{H_0^{LSD}}$*: The local geographic layout has no systematic effect on the variance.*
$\boldsymbol{H_1^{LSD}}$*: The local geographic layout causes local over- or underdispersion.*

The null model assumes that the local variance is unrelated to the geographic arrangement. If the null is accepted, it means that the investigated data gives no indication that geographical factors are responsible for the variance effects. Note that variability can still be related to its particular location. The average level of variability is still treated as a function of location. This is achieved through a local average residual h_i (see Equation 5). However, LSD tests the local spatial influence on the dispersal behaviour above the general local variability level. In conceptual terms, the hypothesis testing scheme of H_0^{LSD} and H_1^{LSD} derives from a linear autoregressive framework. Let $\mathrm{E}_i = \left(\left|e_j\right|^a\right)_j$ with $j \in \mathcal{N}_i$ be a vector of exponentiated residuals from a local neighbourhood i with e_j as defined in Equation (1). Let $\alpha_i = E\left[\left|e_j\right|^a\right]$ be the expected (non-geographic) exponentiated residual within a local neighbourhood i. The two presented hypotheses can be derived from a linear regression model:

$$\mathrm{e}_i = \alpha_i + \rho_i W_i^T \mathrm{E}_i + \varepsilon_i, \tag{4}$$

where e_i denotes the mean deviation influenced by geographical factors, ε_i captures the regression residuals and W_i is the vector of spatial weights for spatial unit i. The null

model occurs when the coefficient ρ_i is close to zero. Hence, LSD tests to what degree this coefficient deviates from zero. If a left-side test is conducted, the alternative model represents a significantly negative ρ_i. Its acceptance thus means that the geographic arrangement, as defined through W, reduces the variance more than it would be the case when geographical factors have no effect. By analogy, acceptance of the alternative in a test on the right-side indicates a significantly positive magnitude of ρ_i, which means that the local geography increases the variability within the random variables. The hypotheses outlined here are thus useful devices to test the role of geographic layout in the local dispersal behaviour of the spatial random variables.

4.2 Mathematical definition

The LSD measure is formulated mathematically as a ratio of the spatially weighted local residuals and their own spatially randomised local average. Therefore, LSD is given by

$$LSD_i = \frac{\sum_{j \in \mathcal{N}} w_{ij} |e_j|^a}{h_i \sum_{j \in \mathcal{N}} w_{ij}}, \quad h_i = \frac{\sum_{j \in \mathcal{N}_i} |e_j|^a}{n_i}, \tag{5}$$

where n_i denotes the cardinality of $\mathcal{N}_i$ and h_i is the local mean residual. Residuals e_j are as defined in Equation 1. The term h_i is a replacement of h_1 and allows a strictly local analysis to be conducted. The datasets can thus be heterogeneous with regard to mean and variance. This important difference from LOSH is further illustrated through the relationship between LOSH and LSD (Appendix A):

$$LSD_i = \frac{H_i \cdot h_1}{h_i}. \tag{6}$$

Equation (6) shows that LSD is a rescaled version of LOSH. Whenever h_i equals h_1, LOSH and LSD are equivalent. This is the case when the local variability equals the global average dispersal behaviour. LSD is particularly valuable when $h_i < h_1$, because LOSH tends to overlook these kinds of weak local structures. In contrast, LSD adapts to specific local conditions and enables truly local variance patterns to be investigated. On the contrary, local deviations detected by LOSH are, at least in part, caused by global instability in the first two moments.

An intrinsically local perspective of LSD is useful in a wide range of situations: i) it can be adopted to describe variegated geographic phenomena occurring at the same time; ii) it allows regions with similar spatial dispersal mechanisms to be revealed beyond the variance magnitudes; iii) it can support in constructing hypotheses regarding the causal mechanisms of phenomena that are spatially coincident; and iv) it is a diagnostic tool for investigating local non-stationarities. Interpreting LSD and LOSH together should provide a clearer insight into spatial variance patterns: LOSH discloses and maps the overall global variance volatility including distinctive boundaries, whereas LSD is able to discover the local patterning mechanisms that influence heterogeneity in a given place. Section 6 demonstrates some of these possible uses.

5. Inference procedure

Two issues complicate the task of making inferences about LSD: potential deviations from normality and the constraint of having to keep the inference local. In the case of normal attributes, LSD can technically be evaluated as a χ^2 test, even though the mean and variance might vary (Walck 2007, p. 38). However, in the light of the results of Xu et al. (2014), we do not want to restrict the test to normal populations that seldom occur in real geographic conditions. Furthermore, the intended local nature of an inference approach might cause problems by the small-size local samples. This is particularly the case when the analytical scale is small. In such cases, there is a serious lack of data available for local resampling and bootstrap distributions are unreliable. The χ^2 approach is thus not applicable and a different inferential strategy is required.

A two-step approach is put forward as a means of overcoming this difficulty:

(1) A Bayesian prediction of synthetic data to increase the size of the local database through
    (a) determining suitable prior distributions and
    (b) a Bayesian updating for adjusting priors to local conditions.
(2) Arranging of local bootstrap distributions using the data from step 1.

The Bayesian approach in the first stage is used to boosting the amount of available data. The purpose of this is to predict additional local mean values, from which auxiliary residuals can be generated. These can then be plugged into LSD during the Monte Carlo iterations in the bootstrap. The second stage describes the final estimation of a reference distribution that is used for inference purposes. The following sub-sections outline these two stages in more detail.

5.1 Bayesian mean prediction

The first part in the inferential approach is to supply the available local subsets with additional information. This is carried out by predicting the synthetic mean values that are used for drawing additional local residuals. The mean estimation is subject to the central limit theorem. This allows us to exploit the advantage of well-known a priori knowledge about the underlying distributional characteristics of mean estimations. Arithmetic means converge to normal distributions. Predicting the means is thus conceptually simpler than drawing the residuals, and for this reason, we have chosen to follow this path rather than predicting residuals directly.

The synthetic means are constructed through a semi-global empirical Bayesian procedure that takes advantage of two sources of information: global information from the overall dataset and local information from the neighbourhoods under consideration. Our proposed approach utilises the observed sampling variability of all the observed mean estimations as prior belief. This global prior reflects strongly averaged information. Hence, the prior belief is further adapted to local conditions by taking account of the local features. The latter step mitigates the global averaging and fits the distribution better to the local conditions in a particular location. In other words, the

outlined two-step approach reduces the risk of adapting to local situations too far by taking into account the global setting (note that observed data might represent outlier situations). At the same time, the approach does not entirely rely on global average information.

The partial inclusion of global information contradicts the stated objectives of LSD. However, the use of global data in the auxiliary Bayesian stage, which precedes the arranging of bootstrap distributions, is a pragmatic compromise and its influence should be kept to a minimum. Apart from predicting means, the global information is not transferred to other parts of the inference procedure such as the bootstrap. The alternative to using global information would be an objective Bayesian approach with an uninformed prior. However, this could result in an excessively overfitted predictive posterior distribution as such approach implies only using local information. In other words, the problems of uninformed objective priors parallel those of local bootstrapping without generating any additional information. An objective Bayesian approach would thus not address the two major issues outlined earlier. The following two sub-sections describe the design of the prior distribution and of the updating step.

5.2 An informed prior

The first stage of the Bayesian predictive approach is to construct a prior that models previous knowledge about the sampling variability of local spatial mean values. The prior must maintain realism, but, at the same time, it should not interfere with the likelihood of the local data that is used in the posterior. That latter likelihood will be obtained from information from the neighbourhood of interest, which must thus then be kept for the updating step. The dual use of data might otherwise lead to a dominant prior that drives the posterior too far, especially with small datasets (Berger 2006, Darnieder 2011, Gelman *et al.* 2013). The dataset is therefore subsetted. In addition to $\mathcal{N}$ and $\mathcal{N}_i$, we define

$$\mathcal{N}_{i+} = \{k \in \mathcal{N} \mid \exists j \in \mathcal{N}_i : w_{jk} \neq 0\}, \quad \mathcal{N}_i \subseteq \mathcal{N}_{i+} \subseteq \mathcal{N}, \tag{7a}$$

$$\mathcal{A}_i = \mathcal{N} \backslash \mathcal{N}_{i+}. \tag{7b}$$

Subset $\mathcal{N}_{i+}$ (Equation 7a) includes the neighbours of the neighbours of unit i. Set $\mathcal{A}_i$ (Equation 7b) contains all the units outside the extended neighbourhood $\mathcal{N}_{i+}$. Figure 1 illustrates these subsets.

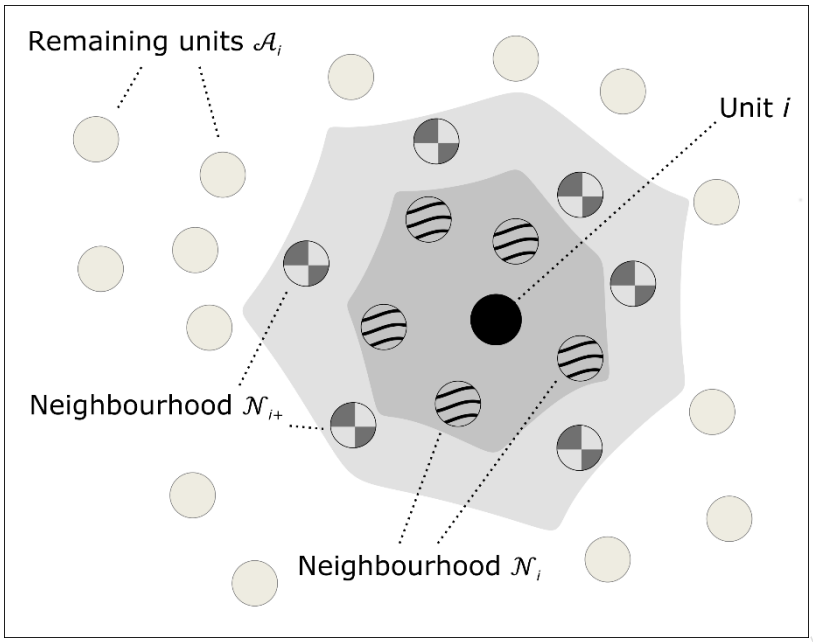

Figure 1. Schematic illustration of region $\mathcal{N}$ separated into $\mathcal{N}_i$, $\mathcal{N}_{i+}$ and $\mathcal{A}_i$.

Constructing an informed prior requires *a priori* distributional knowledge. While making the allowance for global non-stationarity, it is not guaranteed that the underlying random variables X_j will be distributed in an identical manner. However, through the central limit theorem and assuming the sample size to be reasonably large, it can be assumed that the spatially weighted mean values $Y_j = \sum_{k\in\mathcal{N}_j} w_{jk}x_k / \sum_{k\in\mathcal{N}_j} w_{jk}$ are approximately normal. We thus have $Y_j \sim \mathrm{N}\left(\mu_{X_j}, a_j\sigma^2_{X_j}\right)$, where $\mu_{\mathrm{X_j}}$ and $\sigma^2_{\mathrm{X_j}}$ are the unknown expectation and variance of the variates $X_{\mathcal{N}_j}$ (i.e., the variates from $\mathcal{N}_j$). The factor $a_j = \sum_{k\in\mathcal{N}_j} w^2_{jk}/W^2_j$ (see Appendix B) reflects the geographic constraints from the spatial weights matrix W. We can ignore this latter constant for the moment but will need it later in the bootstrap.

We seek to predict the parameters $\mu_{\mathrm{X_j}}$ and $\sigma^2_{\mathrm{X_j}}$. It must be remembered that the prior should be backed up by a sufficient amount of data. Instead of estimating the parameters multiple times from small neighbourhoods, our aim is to combine all the information from $\mathcal{A}_i$. Since $\mathcal{A}_i$ varies across locations, individual priors must be obtained for each neighbourhood. The combined mean and variance estimators are given by (see Appendix C):

$$\bar{x}_c = \frac{\sum_{j\in\mathcal{A}_i} n_j \cdot \bar{x}_j}{\sum_{j\in\mathcal{A}_i} n_j} \quad \text{and} \quad s^2_c = \frac{\sum_{j\in\mathcal{A}_i}(n_j-1)\left(s^2_j+\bar{x}^2_j\right)}{\left(\sum_{j\in\mathcal{A}_i} n_j\right)-n_{\mathcal{A}_i}} - \bar{x}^2_c. \tag{8}$$

These estimators account for mutually overlapping spatial neighbourhoods. Variable $n_{\mathcal{A}_i}$ is the cardinality of $\mathcal{A}_i$ and subscript c illustrates the combinatorial nature of the proposed estimators from Equation (8).

The prior is the product of the two marginal densities of mean and variance outlined above. The mean of Gaussian random variables Y_j is itself a normal random variable centred on $\mu_0 = \bar{x}_c$ and depends on knowledge of the variance:

$$\mu_{X_j} | \, \sigma^2_{X_j} \sim N\left(\mu_0, \sigma_0 = \frac{\sigma^2_{X_j}}{n_i}\right). \tag{9}$$

Technical, but non-substantive parameters (i.e., hyperparameters) are indicated by subscript *0*. Variable n_i gives the measurement scale of the neighbourhood i of interest. We use n_i rather than the scale that is actually associated with $\bar{x}_c$ to increase the realism of the prior. The much larger cardinality of $\mathcal{A}_i$ would otherwise cause the prior to be underdispersed. The influence of the prior on predictions could then become overly dominant. Employing n_i instead, is a means of matching the prior scale to that of the neighbourhood of interest and is thus more appropriate.

The variance $\sigma^2_{X_j}$ follows a normal scaled inverse-chi-squared distribution (Gelman et al. 2013, p. 67f.). This results from the χ^2-distributed scaled ratio of the sample variance to the variance of the population:

$$\frac{(n_i - 1) \cdot s_c^2}{\sigma^2_{X_j}} \sim \chi^2_{n_i - 1} \;\Rightarrow\; \sigma^2_{X_j} \sim \chi^{-2}_{scaled}(\upsilon_0, \tau_0^2). \tag{10}$$

As in the case of the mean, the degrees of freedom υ_0 is adjusted to $n_i - 1$ instead of $(\sum_{i=1}^{n} n_i) - n$, as it is necessary for the prior to be informative about predicting data for $\mathcal{N}_i$ rather than $\mathcal{A}_i$. The scale parameter τ_0^2 is equal to the variance estimate s_c^2.

A combination of the two marginal densities from Equations (8) and (9) yields the prior (see Appendix D)

$$\pi(\mu, \sigma^2) \propto \frac{1}{\sigma^{3+\upsilon_0}} \cdot \exp\left(-\frac{n_i(\mu - \mu_0)^2 - \upsilon_0 \tau_0^2}{2\sigma^2}\right). \tag{11}$$

This prior represents the non-spatial global *a priori* belief about mean values estimated from samples of size n_i. It thus represents information about the variability of mean estimations from across the entire study area beyond location i of interest. Figure 2 provides a parameterised illustration of the constructed prior density.

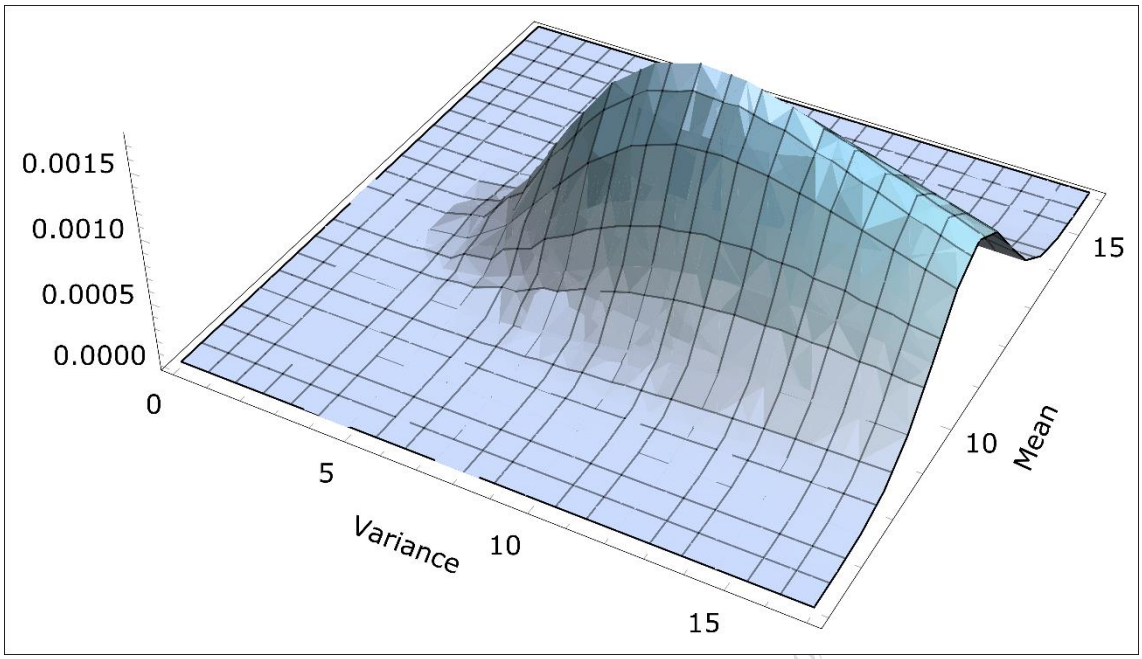

Figure 2. Illustration of the prior density for $n_i = 10,\ \mu_0 = 11,\ \upsilon_0 = 5$ and $\tau_0^2 = 16$.

5.3 Posterior distribution

The posterior combines the prior with the likelihood of the observed local spatial mean value $Y_i \sim N\left(\mu_{X_i}, a_i\sigma_{X_i}^2\right)$. Our aim is to predict suitable values for μ_{X_i} and $\sigma_{X_i}^2$. These parameters specify the final Gaussian from which the additional means are drawn. Constant a_i is, again, fixed because it is a non-random property of the neighbourhood of interest. The respective posterior follows a normal scaled inverse-chi-squared distribution and yields (see Appendix E)

$$f\left(\mu_{X_i}, \sigma_{X_i}^2 \mid Y_i\right) \propto \frac{1}{\sigma_{X_i}^{4+\upsilon_0}} \cdot \exp\left(-\frac{n_i\left(\mu_{X_i}-\mu_0\right)^2+\left(Y_i-\mu_{X_i}\right)^2+\upsilon_0\tau_0^2}{2\sigma_{X_i}^2}\right). \tag{12}$$

Drawing values for μ_{X_i} and $\sigma_{X_i}^2$ requires deriving the conditional posterior $\mu_{X_i} \mid \sigma_{X_i}^2, Y_i$ and, since this in turn requires a known $\sigma_{X_i}^2$, the corresponding marginal posterior $\sigma_{X_i}^2 \mid Y_i$. By building on the results obtained from Gelman et al. (2013), we derive

$$\mu_{X_i} \mid \sigma_{X_i}^2, Y_i \ \sim\ N\left(\frac{\mu_0+Y_i}{2}, \frac{\sigma_{X_i}^2}{2n_i}\right), \tag{13a}$$

$$\sigma_{X_i}^2 \mid Y_i \ \sim\ \chi_{scaled}^{-2}(\upsilon_0 + n_i, \tilde{\tau}^2) \quad \text{and} \quad \tilde{\tau}^2 = \frac{\upsilon_0\tau_0^2+(n_i-1)s^2+\frac{n_i}{2}(Y_i-\mu_0)^2}{\upsilon_0+n_i}, \tag{13b}$$

where s^2 is the sample variance from neighbourhood $\mathcal{N}_i$. The conditional mean posterior in Equation (13a) is a trade-off between prior belief and observed local information. Its mean averages the combined means, while its scale shows that the

posterior is supported by twice the amount of information, as it is based on two separate mean estimations. The marginal variance posterior in Equation (13b) has additive degrees of freedom, whereas the updated scale parameter $\tilde{\tau}^2$ combines the prior and observed sum of squares. The latter are dilated by extra uncertainty from the deviation between the combined means. While the two individual sums of squares in the numerator represent the variability within the individual distributions, the additional uncertainty stems from the likelihood of both occurring together.

Equations (13a) and (13b) demonstrate that the prior and the local information each supply half of the posterior information. The benefit of this is that the posterior is robust against inflation, which might be caused by local boundary conditions or by extreme global imbalance.

5.4 Bootstrapping

The final methodological stage is to generate a bootstrap distribution for LSD that involves the Bayesian procedure outlined above. In each bootstrap iteration, the following steps must be repeated:

(1) random resampling with replacement within the local neighbourhoods,
(2) drawing of new synthetic means and recalculation of the residuals,
(3) recalculation of LSD for each drawn pseudo-sample with substituted means,
(4) estimation of an empirical distribution of LSD and assessment of pseudo p-values p^*.

These four stages resemble the Monte Carlo approach outlined in (Hope 1968). A concise description of the stages that are usually involved in this kind of approach, is also found in (Dray 2011, p.129f.). What differentiates our approach from these two studies is that the proposed bootstrap is locally constrained. The drawing of additional means in Stage 2 involves the Bayesian approach from Sections (5.2) and (5.3) and is achieved in three phases:

(1) drawing of a posterior variance $\sigma_{X_i}^2$ from Equation (13b),
(2) substitution of $\sigma_{X_i}^2$ into Equation (13a) and drawing of a posterior mean μ_{X_i},
(3) drawing of new mean values from $N\left(\mu_{X_i}, a_i\sigma_{X_i}^2\right)$.

The pseudo p-values p^* that are needed for inference can then be calculated in different ways, depending on the desired hypothesis testing scheme (Table 1).

Table 1. Overview of estimators of pseudo p-values p^* for different types of hypotheses. LSD_{i_0} denotes an observed LSD value, LSD_{i_k} is the LSD value obtained from the k-th bootstrap, m is the overall number of iterations and α is the adjusted significance level. We use # to denote the cardinality of a set to avoid notational ambiguity.

Testing scheme	Pseudo p-value estimator	Interpretation of $p^* < \alpha$
Right-tailed	$p^* = \frac{1}{m}\#\{k \mid LSD_{i_k} > LSD_{i_0}\}$	Geographic arrangement increases the variance
Left-tailed	$p^* = \frac{1}{m}\#\{k \mid LSD_{i_k} < LSD_{i_0}\}$	Geographic arrangement reduces the variance
Two-tailed	$p^* = \frac{1}{m}\#\{k \mid LSD^*_{i\,k} > LSD_{i_0}\}$, where $LSD^*_{i\,k} = \left\lvert LSD_{i_k} - \overline{LSD_{i_k}} \right\rvert$	Geographic arrangement affects the variance

6. Empirical results from a LiDAR-derived dataset

Both LSD and LOSH are applied to a subset of 4,436 height differences calculated from two co-registered and filtered LiDAR datasets between 20th and 24th August 2016. These are taken from an 'automatic terrestrial laser scanning station' (ATLS) monitoring project of daily scans, which involves surveying a slow-moving landslide in Gresten, Austria (Figure 3, c.f. Canli *et al.* 2015, Höfle *et al.* 2016). The height differences were obtained from the 'Multiscale Model to Model Cloud Comparison' (Barnhart and Crosby 2013, Lague *et al.* 2013), a point-based comparison method that recognises the existence of sampling variability and measurement error. The eastern part of the scanned area got mown in between the two dates (a figure showing the study area before and after the mowing is provided in the online supplementary material). The dataset thus comprises a distinctive global structure (mown vs. unmown; diagonal dividing line) and, in addition, weaker local structures within the sub-regions. This two-stage structure makes the data a suitable test case for LSD and LOSH. These techniques are applied with inverse-distance weighting and a cut-off at a distance of one meter. This scheme is useful because the observed process has a positive spatial autocorrelation and does not show abrupt changes within the regimes. Note that the obtained results should not be understood as outcomes of an empirical investigation, but rather as a scenario for demonstrating differences between LSD and LOSH.

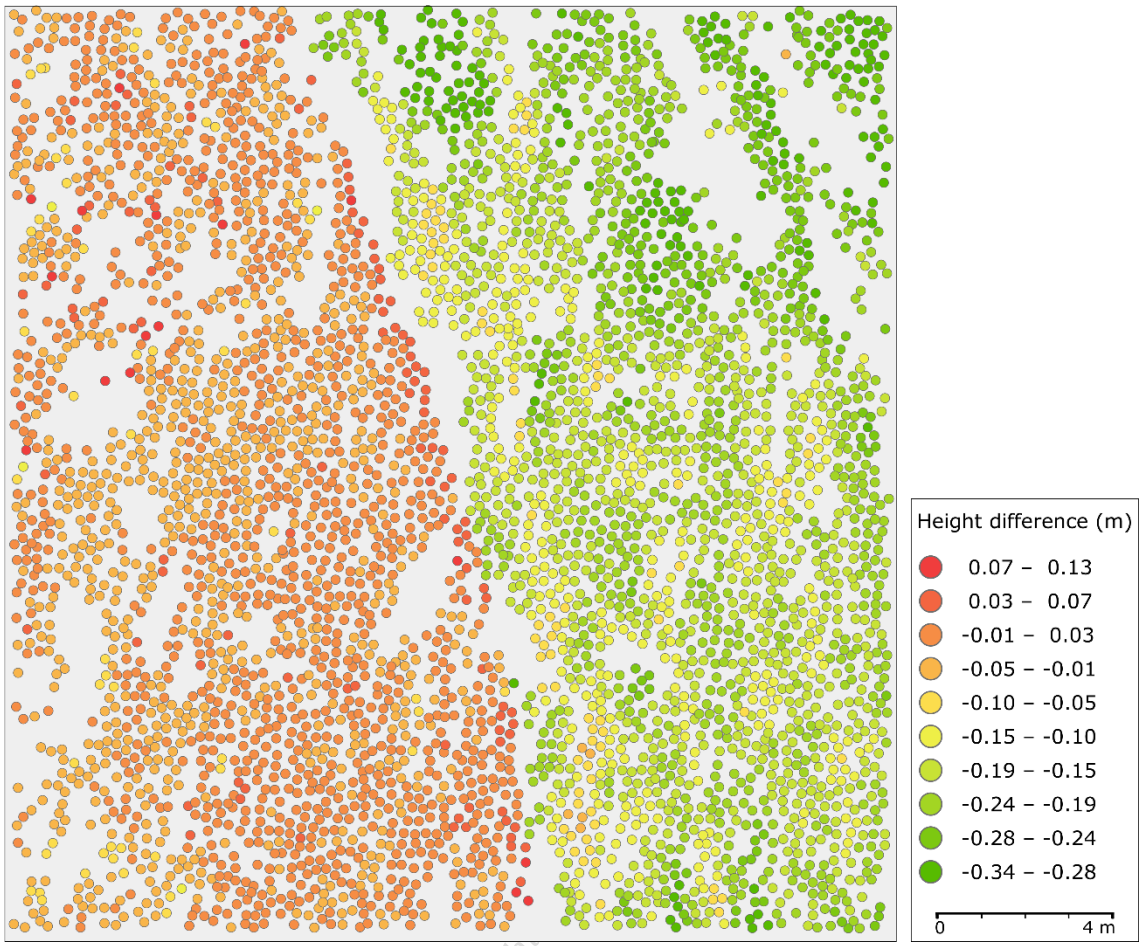

Figure 3. Height differences between two ATLS datasets.

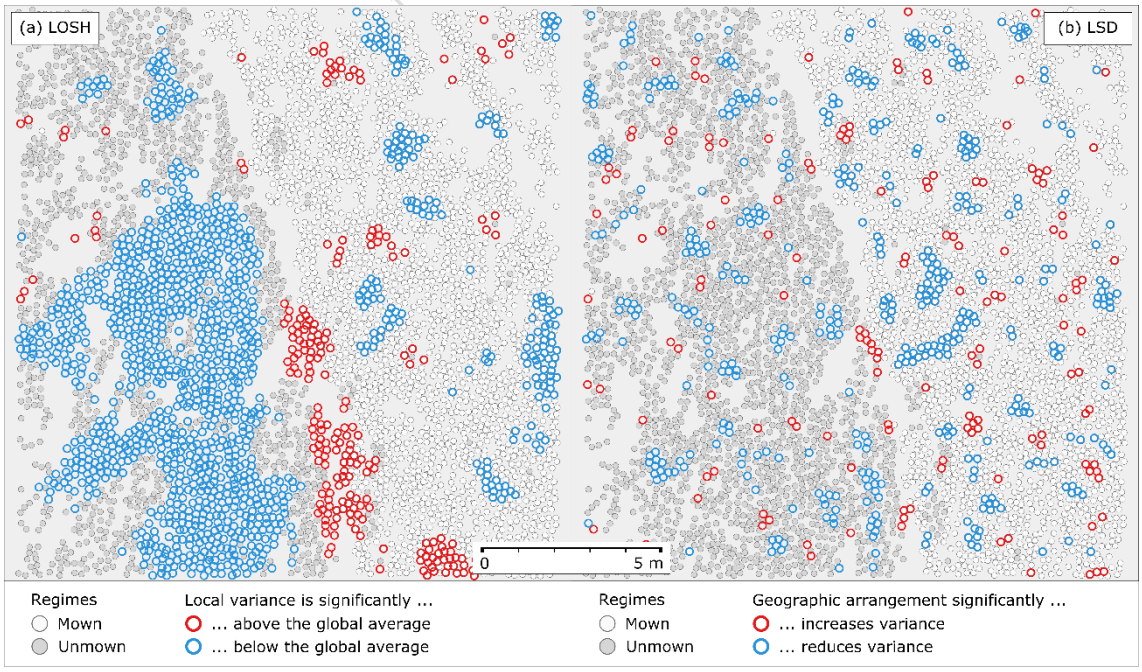

Figure 4. Significant scores from (a) LOSH and (b) LSD (two-sided test; $\alpha = 0.05$; 1,000 iterations).

6.1 Interpretation of LSD and LOSH

The results from LSD and LOSH reveal different features of variance patterns. Thus, when they are interpreted together, it is easier to make a direct comparison. Figure 4 maps statistically significant LOSH and LSD outcomes. We randomise locally, but omit the Bayesian approach for the moment, as all the involved neighbourhoods are sufficiently large. The smallest available neighbourhood size is $n_i = 8$, which allows $8! = 40{,}320$ permutations. The average of $n_i = 54$, however, allows ca. 2.31×10^{71} permutations, which is enough for virtually all the application scenarios. Despite this, $n_i = 8$ is still a small number of observations and hence contains little information. The Bayesian technique thus proves to be useful, as will be discussed in Sub-section 6.5.

The global dividing line cutting across the centre of the region, is a feature where significant LOSH values from the right tail of the reference distribution accumulate (Figure 4a). Thereby, the southern part dominates, while the northern part of the line is influenced by a spatial gap (a gentle slope in the terrain) which is an obstacle to high LOSH scores. Further high values are found in the mown regime, in particular in the northernmost part (disturbances from artefacts) and in the South (these vanish when the false discovery rate is controlled by following Benjamini and Hochberg (1995)). In contrast, the western unmown part is dominated by significantly low LOSH values. These are caused by the global resampling scheme of LOSH, which shifts statistically differing values from the mown part into the unmown region. This biases the p-values towards the left tail of the bootstrap distribution and makes it impossible to disclose local variance patterns. The eastern mown regime is not as homogeneous as expected. Grass cuttings produced from the lawn mower were being left on the meadow. This increases the global average residual h_1 and in turn leads to a more homogeneous appearance of the unmown regime, as explained earlier. Nevertheless, LOSH reveals and maps the global variance structure in the locality by identifying the most (the dividing line) and least dispersed areas (the unmown part).

The LSD values (Figure 4b) are more evenly distributed than the LOSH values. Unexpectedly and in stark contrast with LOSH, the dividing line no longer appears on the map except for a small part in the centre. The local spatial arrangement is thus not leading to the variability of the features and it can be concluded that the dividing line is a truly global feature that is only caused by the existence of two different regimes. Apart from this, the western part is no longer as homogeneous as it appeared with LOSH. LSD reveals certain significant local features that are interspersed and like small spots of high variability within the unmown part. The overall distribution of the LSD values is, however, rather homogeneous across the two regimes (Table 2). The structures in the mown and unmown parts therefore do not seem to differ noticeably and behave in a relatively similar way. A different significance evaluation will be seen when the Bayesian mean prediction is incorporated in Sub-section 6.5.

Table 2. Descriptive statistics for LSD scores within the mown and unmown regimes.

Regime	Min	Max	Mean	Median	Standard deviation	Interquartile range
Mown	0.146	3.185	0.907	0.823	0.363	0.446
Unmown	0.249	4.426	0.904	0.782	0.453	0.501

In summary it can be stated that an evaluation of LOSH and LSD scores in combination reveals both global and local variance patterns. The observed LSD values further confirm that, at least for the adjusted analytical scale, the dividing line is a global feature. It is also clear that local structures that remain hidden with LOSH are present in the map when LSD is considered. The LSD scores thus provide an additional insight into the dataset.

6.2 A map of global and local spatial variance patterns

It is worth flagging the significance of the LSD and LOSH values, but they are not exhaustive in terms of their interpretation. The maps in Figure 5 thus provide a classification scheme for LOSH-LSD tuples. Four standard gradients can be derived from these, each characterising different sub-regions in the map.

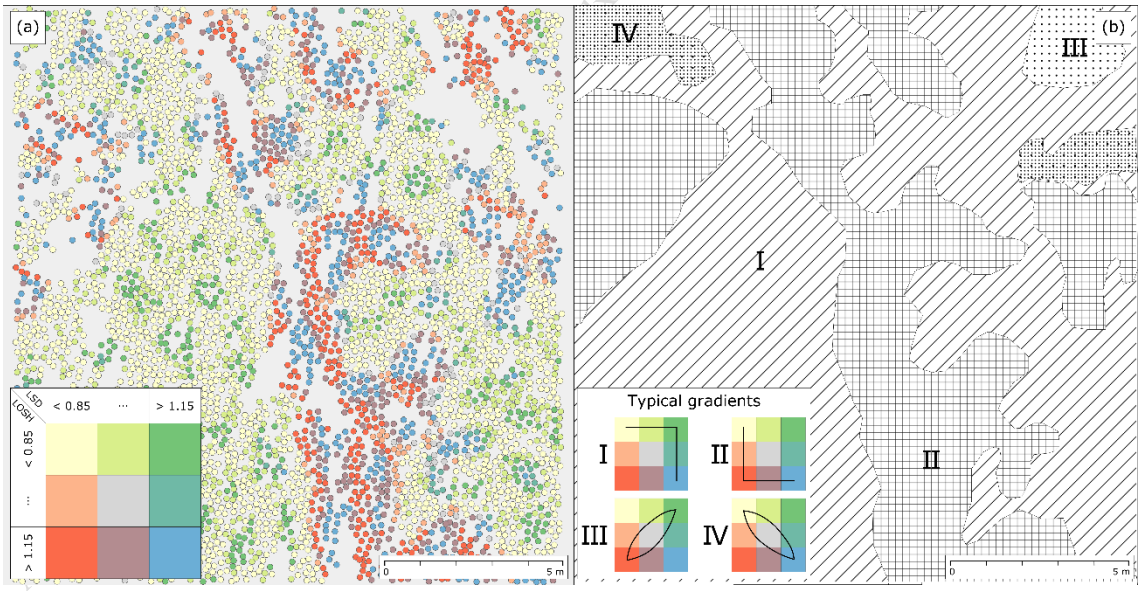

Figure 5. Variance patterns within LiDAR-derived height differences. (a) A detailed characterisation of local and global effects: the variance can be above the global mean and increased at a local level by the geographic pattern (blue) or below the global mean and reduced further at a local level at the same time (yellow). The locations can also be homogeneous from a global standpoint while the local pattern increases the variance (dark green) or vice versa (red), with all sorts of possible transitional effects (intermediate colours); (b) A schematic sketch of LOSH-LSD configurations: the prevailingly local structures (I), the prevailingly global structures (II), locally homogeneous, and globally dispersed (III), global and local variance fluctuations (IV).

Figure 5 shows a way to classify LOSH and LSD outcomes together. A prominent feature in Figure 5a is, again, the dividing line (see also Type II gradient in Figure 5b). The figure, however, shows the line in more detail: The centre of the line appears to be narrow and elongated and reflects the thin crisp edge of the boundary where the two regimes meet. The spatial pattern strongly increases the variance in this from both a global and local standpoint. Adjoining this is a fuzzy region where local spatial effects are negligible, while the spatial variance is generally high in a global comparison. In other words, while the global variance gradient features prominently, the local spatial variance pattern is closer to randomness and regularity. The local geographic arrangement is thus not related to the increased variance in these regions.

When one moves farther away from the dividing line, the effects prevail at a local level. The variance structures turn into insular regions of small areas where the local pattern increases the variance, which are surrounded by a homogenising geographic arrangement (Type I). The northern part, which is affected by artefacts, is further characterised by two volatile variance patterns (Types III and IV). The Type III pattern, which is featured in the north-eastern part, is caused by a larger haystack. This appears to be regular in local terms (its internal structure), but is disruptive globally as it is a prominent feature (above the global mean variance). In contrast, the Type IV pattern reflects taller bunch grass that is characterised by abrupt fluctuations between regular and heterogeneous conditions caused by the related clumps of culms. An interpretation that combined LOSH and LSD made it possible to distinguish these rather different features in the data.

The detailed interpretations given above, demonstrate the additional value that LSD provides. Global structures are detected and mapped locally by LOSH where these dominate, but local details are missed out. In contrast, LSD assesses local structures and describes in greater detail the internal structure of global features (e.g., the nature of the central boundary or of the homogeneous sub-regions). The measure thus not only assesses different structures, but also reveals additional information about features obtained from LOSH.

6.3 Interplay with variance

Since both LSD and LOSH are measures of variance, it is worth investigating how they relate to the magnitude of the non-spatial local variance. This illustrates the ability of LOSH and LSD to separate effects of spatial patterning from other influences of general variability.

The design of LOSH implies there is a strong dependence on general local variability through its constant denominator. When a sub-region is generally diverse, the prospect of assessing high LOSH scores is also high, regardless of the local spatial patterning. Figure 6a illustrates this link, and Kendall's Tau-b, an ordinal correlation measure that accounts for non-normality and ties, gives further support through a strongly significant test score of $\tau = 0.679$ ($p < 0.001$). However, this relationship is not uniform since LOSH is more dispersed when the local variability is stronger. Regressing LOSH on variance and conducting a non-parametric Koenker-Bassett test

(Koenker and Bassett 1982, Godfrey 1996) on the residuals, confirms the heteroscedasticity that is visible in Figure 6a. The two diverging quartile trend lines in the biquantile regressogram (Figure 6b) underpin this outcome, while the median trace shows that variance is a good predictor of LOSH. The measure is thus dominated by non-spatial variability. This result is in accordance with the intended purpose of LOSH to detect both the most and least dispersed regions in geographic data. However, it also shows that LOSHs power to detect solely spatial effects in local circumstances is limited.

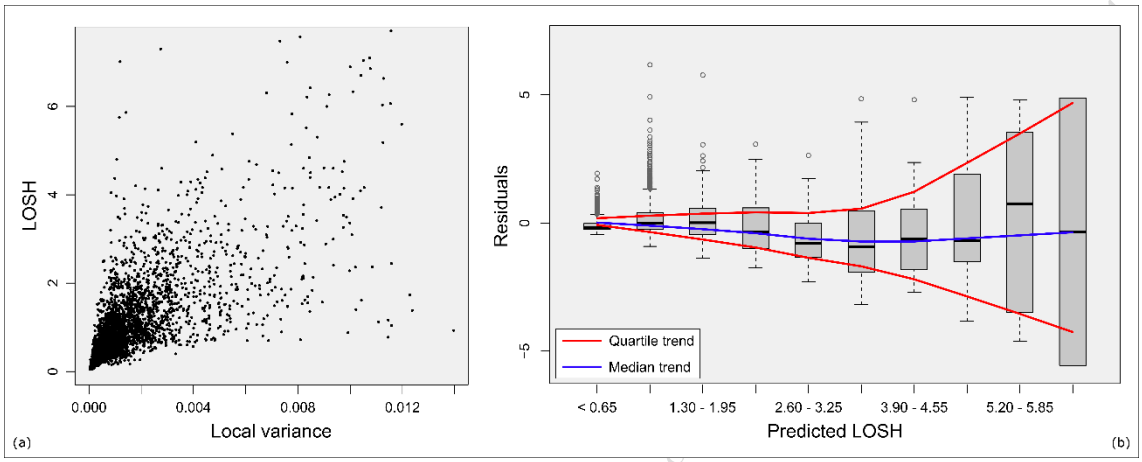

Figure 6. Relationship between LOSH and local variance. (a) A scatter plot of variance and LOSH; and (b) A biquantile regressogram (Tukey 1977) illustrating heteroscedasticity in LOSH.

In contrast, Figure 7a shows that LSD is only weakly related to variance ($\tau = 0.023,\ p < 0.001$), and the median trend line in the regressogram (Figure 7b) represents a relationship that varies with the strength of LSD. Variance is a sufficient predictor of LSD when it is strong and when, at the same time, the influence of the spatial patterning is weak (i.e., the right part of the scatter plot in Figure 7a). However, the ascending slopes of the median, as well as the quartile trend lines (Figure 7b) show that variance systematically overestimates high LSD scores. The spatial pattern thus dominates the (more interesting) high LSD values. These characteristics are desirable properties: LSD only has a negligible link with local variance, while extremal outcomes are controlled by the spatial effects that they are supposed to quantify.

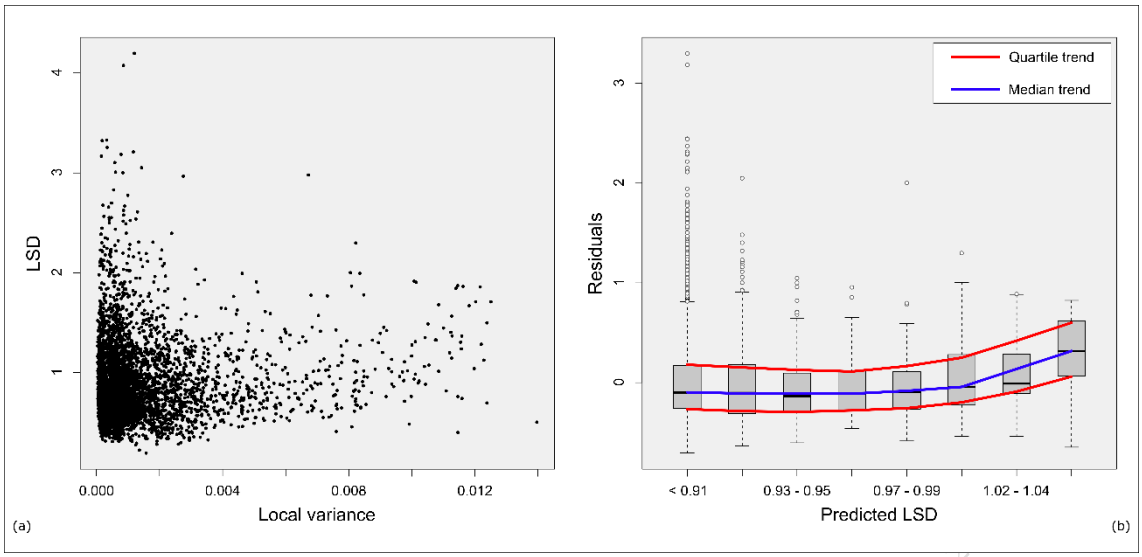

Figure 7. Relationship between LSD and local variance. (a) A scatter plot of variance with regard to LSD; and (b) a biquantile regressogram (Tukey 1977) illustrating heteroscedasticity within LSD.

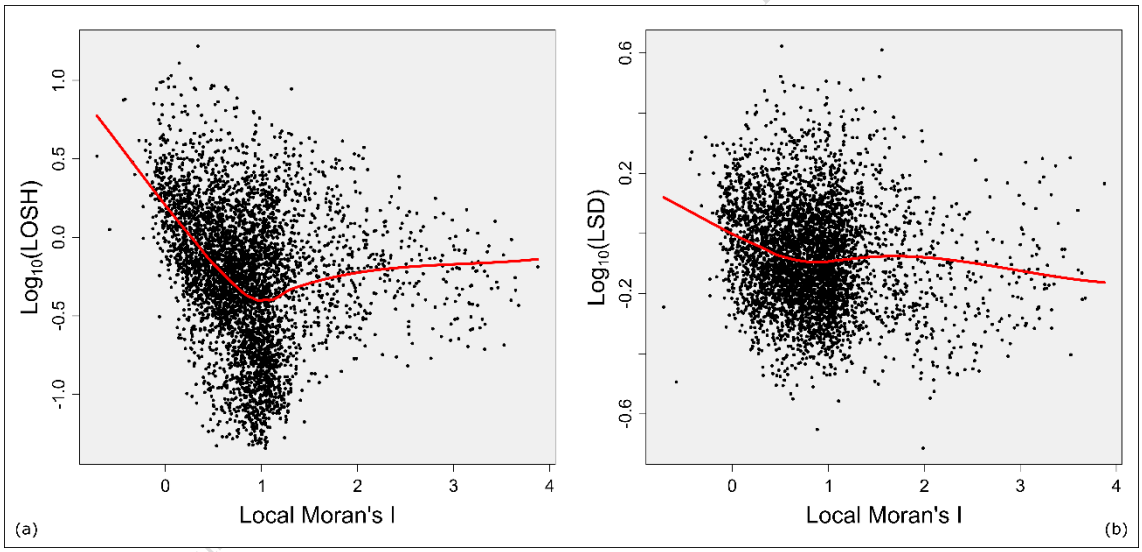

Figure 8. The relationship of LOSH and LSD with local Moran's I. The logarithms of the two measures were chosen to improve interpretability. The red line represents a first-order LOESS trend. (a) LOSH; and (b) LSD.

6.4 Relationship with spatial autocorrelation

The two measures quantify different aspects of 'dissimilarity' within random variables. As mentioned in Section 2, spatial autocorrelation represents an additional, covariance-based dimension of heterogeneity. Local estimators like local Moran's I (Anselin 1995) can be used to quantify spatial autocorrelation, and Figure 8a shows its relation to LOSH. The Moran interval [0.0, 1.4] shows a significant negative relationship ($\tau = -0.27$). LOSH is high when the association between neighbours is random and low when observations occur in a clustered form. Both measures therefore, to some extent,

highlight similar structures from different perspectives (variance vs. covariance). Observations showing autocorrelations higher than 1.4 belong to the northern artefacts and thus can reasonably be regarded as outliers, that do not conform to the general observations made above. Overall, LOSH reveals roughly similar structures to those of Moran's I, as is evident from their antipodal behavioural pattern.

In contrast, LSD is almost unrelated to Moran's I, when the latter is on the interval [0.0, 1.4]. Most of the data points accumulate on the left side of the scatter plot in Figure 8b without showing any notable trend ($\tau = -0.09$). This strengthens the likelihood indicated above that LSD is able to reveal patterns that cannot be detected by LOSH and Moran's I. These detected patterns are not linked to the clustering tendency of the attribute values. Rather, they are features in their own right, which makes them of value for empirical investigations since they might supply important details about the disclosure of the mechanisms in spatial random variables.

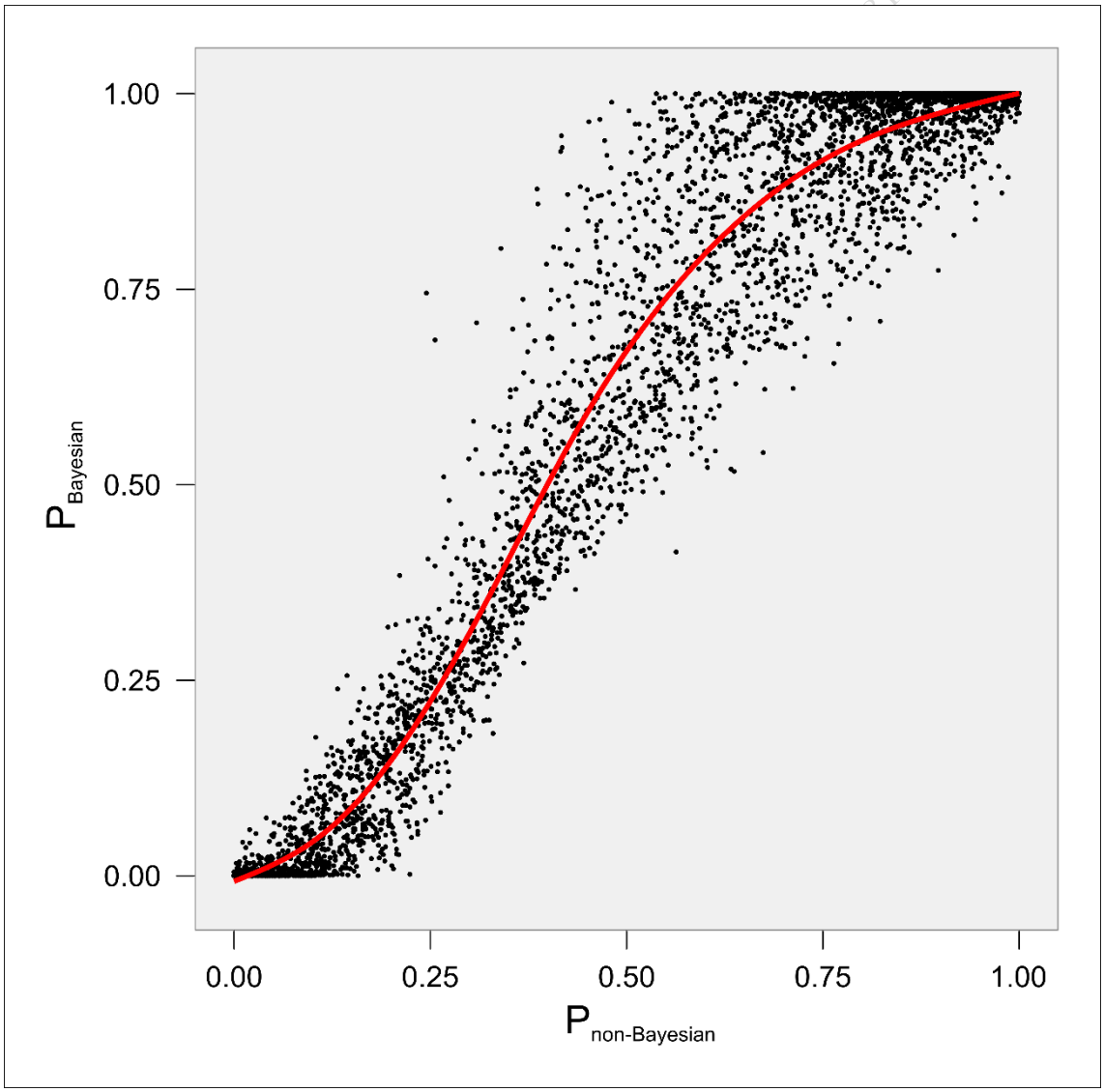

Figure 9. The relationship between the Bayesian and the non-Bayesian p-values.

6.5 Influence of the Bayesian prediction of mean values

The Bayesian procedure from Section 5 extends local resampling by the use of synthetic data generated from empirical prior knowledge combined with local information. This approach differs from conventional bootstrapping that only relies on observed information. There is a need to investigate how the Bayesian approach influences drawn inferences.

Figure 9 shows a sigmoidal relationship between conventional p-values (i.e., those that were used in the previous paragraphs) and those involving synthetic means. They show a strong monotonic association of $\tau = 0.77$ at medium ranges. There is a significant fall in this association in both tails ($\tau = 0.23$), which is an important observation as the tails possess values which are important for drawing inferences. In the Bayesian approach, the p-values tend to concentrate around the extremes of 0 and 1. In contrast, conventional p-values show a higher level of dispersion in the tails. This is caused by the number of available observations, which have limited explanatory power because they only represent a small fraction of all possible values. In contrast, the Bayesian approach extends this spectrum, which increases its ability to detect spatial effects because the comparative values are not biased towards a certain range.

The increased ability to detect effects with the Bayesian approach is further evident after the p-values have been corrected for multiple hypothesis testing. Note that LSD tests n hypotheses with one dataset. This repeated use of the data leads to an increase in the Type I error rate and requires correction. When the false-discovery rate is controlled at $\alpha = 0.05$ (FDR; Benjamini and Hochberg 1995) and the p-values are corrected accordingly, it is seen that the non-Bayesian approach is very conservative. Only 0.5% of all the null hypotheses are rejected, which is way below the significance level that was envisaged. In other words, many actual effects might be missed out. In contrast, when the Bayesian-generated p-values are adjusted, they yield a ratio of 5.2%, which is close to the desired α level.

Figure 10 illustrates the FDR-corrected p-values of significant observations by incorporating the Bayesian-generated means. The significant features in the eastern part (the ‘mown’) show a general North-South bearing (Figure 10a) and resemble the direction of the mowing process, which is illustrated in the background of Figure 10b through a hill-shading raster. The blue features, where the geographic layout reduces the variance, either accumulate alongside the small piles of hay that were left on the meadow or in the furrows in-between. In contrast, the western part (the ‘unmown’) is not affected by the after-mowing topography. The patterns of significant features observed in this part are mostly unrelated to the hill-shading. This makes sense given that the height differences that were analysed are affected by physical, biological and other factors that do not necessarily correspond to the topography shown in Figure 10b, especially in the unmown area.

A comparison of Figure 10 with Figure 4b shows that the conventional p-values generated from the local bootstrapping, do not show the features described above. In fact, there is no noticeable difference between the mown and unmown parts in this case. The p-values generated by the inclusion of predicted means are closer to the

phenomenon (especially in the mown part) and can thus be considered to be of greater value. Hence, this comparison implies that the proposed Bayesian approach is a reasonable alternative to more conventional forms of pseudo p-value estimation.

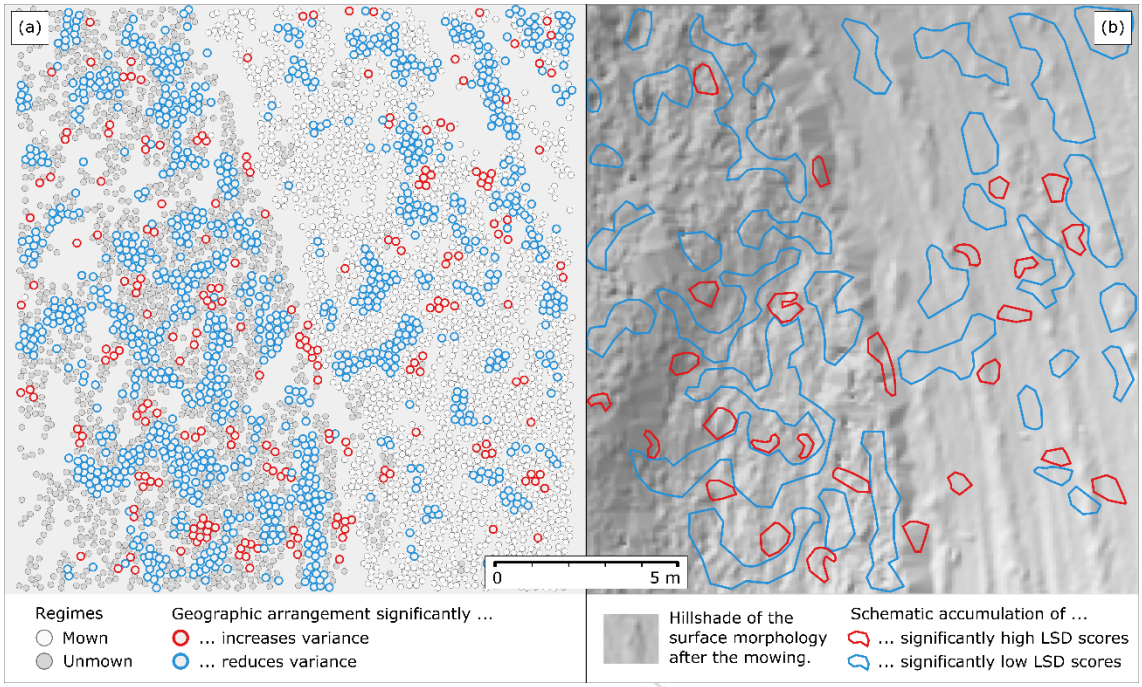

Figure 10. Significant LSD scores involving Bayesian-predicted means (two-sided test; $\alpha = 0.05$; 1,000 iterations). (a) Map of significant features. (b) Schematic sketch of significant accumulated features, against the background of the hill-shading of the surface after the mowing.

7. Discussion and conclusions

This paper introduces a test called 'Local Spatial Dispersion' (LSD), which is able to determine the local influence of geographic arrangements on variance. It does not incorporate global information and allows local patterns to be detected in the presence of a global structure. The strictly local nature of the test, however, increases the risk of problems arising from small-size samples within local neighbourhoods. To mitigate this risk, a stratified bootstrapping procedure is introduced that combines traditional resampling with a Bayesian prediction of synthetic data. The proposed LSD supplements LOSH, which is a recently devised technique to map global variance structures locally. The measure adapts LOSH to strictly local circumstances. Conceptually, LSD forms a part of a series of localised techniques like the hot spot method called 'O-statistic' (Ord and Getis 2001), or locally adaptive geometric clustering techniques such as the inhomogeneous marked and unmarked K-functions (Cuzick and Edwards 1990, Baddeley *et al.* 2000).

Its application to a dataset for height differences derived from LiDAR data demonstrates the ability of LSD to detect local patterns within a distinct global structure. An interpretation combined with LOSH reveals further characteristic variance patterns, which would not have been detected by using either measure alone.

Furthermore, the obtained results show that LOSH is closely correlated with general non-spatial variability, which hampers the separation of genuinely spatial from other effects. In contrast, LSD is uncorrelated with non-spatial variation and is capable of exposing entirely spatial variance effects. Notably, LSD is also unrelated to positive spatial autocorrelation. This allows the measure to assess other complex patterns apart from general attribute clustering, such as the internal structures of clusters and the detailed contours of geographic boundaries. The proposed inference mechanism further facilitates the detection of local structures. While conventional stratified bootstrapping turns out to be overly conservative, the synthetic expansion of the available local data keeps the α-rate in compliance with the adjusted significance level, which increases its ability to detect meaningful patterns. Overall, LSD has been shown to be a useful extension to the spatial analysis toolbox. In the given example, it is possible, in statistical terms, to detect local interaction between variance and spatial patterns within global structures and thus to disclose details that would otherwise have been overlooked.

The anonymous reviewers pointed out that there was a relationship between the proposed LSD technique and local variograms. Variograms quantify the variance of the spatial increment between two locations separated by a certain distance (Bachmaier and Backes 2008, Cuba *et al.* 2012). Both, LSD and variograms are thus concerned with variance estimation. What differentiates them is that LSD is a) a hypothesis test designed to determine the influence of a specific spatial arrangement on variance and b) that it is concerned with in-place variance rather than with the variance of the incremental process. In contrast, variograms estimate variance within certain distance bands by relying on the validity of the employed spatial weights (instead of testing their influence). The estimates of the variograms are then used for modelling (e.g., in Kriging), which means that our proposed test can be used as a diagnostic tool for geostatistics. For instance, LSD can be used to fully investigate the possible sources of local non-stationarities, which might lead to a lack of stationarity in the difference processes between locations. Thus, LSD might also be a useful device in the area of geostatistics.

However, there are some shortcomings in this paper that could not be addressed. One of these is that our data only have a positive spatial autocorrelation. A negative spatial autocorrelation is different in nature, since it involves a certain degree of heterogeneity, which in turn is related to variance. An interesting relation between LSD and negative spatial autocorrelation might thus exist, which would be worth exploring in a systematic way in a future research project. In terms of inference, the forms adopted for the prior and likelihood are strongly supported by the central limit theorem and leave little room for variation. However, the way that the prior and likelihood enter the posterior distribution, need to be analysed with regard to suitable combinations other than the applied ‘half-and-half scheme’. For instance, an adaptive solution could be useful, in which the likelihood is given more weight in larger neighbourhoods that are backed up by a more solid database. In terms of LOSH, our empirical results show a strong heteroscedasticity with regard to local variance. Future research should therefore seek to achieve a variance stabilisation in order to make the outcomes of LOSH more

robust for inhomogeneous populations and assist its interpretation. From a technological standpoint, the proposed solution is computationally expensive as it includes bootstrapping. The application of LSD to large datasets would hence clearly benefit from an efficient implementation strategy. All in all, LSD provides the means of obtaining a valuable and detailed insight into variance mechanisms of geographic random variables and offers the prospect of achieving significant new empirical results in various fields.

Acknowledgements

This work was supported by the *German Research Foundation* (*DFG*) through the priority programme 'Volunteered Geographic Information: Interpretation, Visualisation and Social Computing' (SPP 1894). Special thanks go to *Prof Thomas Glade* (*University of Vienna*) for the provision of LiDAR data from the '4DEMON' project. We would also like to thank the *Lower Austrian government* for their financial support for the LiDAR data collection within the framework of the 'NoeSLIDE' project.

References

Abascal, M. and Baldassarri, D., 2015. Love Thy Neighbor? Ethnoracial Diversity and Trust Reexamined. *American Journal of Sociology*, 121 (3), 722–782.

Anderson, C., Lee, D., and Dean, N., 2014. Identifying Clusters in Bayesian Disease Mapping. *Biostatistics*, 15 (3), 457–469.

Anselin, L., 1988. Lagrange Multiplier Test Diagnostics for Spatial Dependence and Spatial Heterogeneity. *Geographical Analysis*, 20 (1), 1–17.

Anselin, L., 1990. Spatial Dependence and Spatial Structural Instability in Applied Regression Analysis. *Journal of Regional Science*, 30 (2), 185–207.

Anselin, L., 1995. Local Indicators of Spatial Association - LISA. *Geographical Analysis*, 27 (2), 93–115.

Anselin, L., 2001. Spatial Econometrics. *In*: B. Baltagi, ed. *A Companion to Theoretical Econometrics*. Hoboken, NJ: Wiley-Blackwell, 310–330.

Anselin, L., 2010. Thirty Years of Spatial Econometrics. *Papers in Regional Science*, 89 (1), 3–25.

Arnot, C. and Fisher, P., 2007. Mapping the Ecotone with Fuzzy Sets. *In*: A. Morris and S. Kokhan, eds. *Geographic Uncertainty in Environmental Security*. Dordrecht: Springer Netherlands, 19–32.

Bachmaier, M. and Backes, M., 2008. Variogram or Semivariogram? Understanding the Variances in a Variogram. *Precision Agriculture*, 9, 173–175.

Baddeley, A., Moller, J., and Waagepetersen, R., 2000. Non- and Semi-Parametric Estimation of Interaction in Inhomogeneous Point Patterns. *Statistica Neerlandica*, 54 (3), 329–350.

Barbujani, G., Oden, N., and Sokal, R., 1989. Detecting Regions of Abrupt Change in Maps of Biological Variables. *Systematic Zoology*, 38 (4), 376–389.

Barnhart, T. and Crosby, B., 2013. Comparing Two Methods of Surface Change Detection on an Evolving Thermokarst Using High-Temporal-Frequency

Terrestrial Laser Scanning, Selawik River, Alaska. *Remote Sensing*, 5 (6), 2813–2837.

Bavaud, F., 2014. Spatial weights: constructing weight-compatible exchange matrices from proximity matrices. *In*: M. Duckham, E. Pebesma, K. Stewart, and A.U. Frank, eds. *Geographic Information Science: 8th International Conference, GIScience 2014*. Vienna, Austria: Springer Berlin Heidelberg, 81–96.

Benjamini, Y. and Hochberg, Y., 1995. Controlling the False Discovery Rate : A Practical and Powerful Approach to Multiple Testing. *Journal of the Royal Statistical Society: Series B (Methodological)*, 57 (1), 289–300.

Berger, J., 2006. The Case for Objective Bayesian Analysis. *Bayesian Analysis*, 1 (3), 385–402.

Berkes, F., Hughes, T., Steneck, R., Wilson, J., Bellwood, D., Crona, B., Folke, C., Gunderson, L., Leslie, H., Norberg, J., Nyström, M., Olsson, P., Österblom, H., Scheffer, M., and Worm, B., 2006. Globalization, Roving Bandits, and Marine Resources. *Science*, 311 (5767), 1557–1558.

Box, G., 1953. Non-Normality and Tests on Variances. *Biometrika*, 40 (3/4), 318–335.

Bravo, C. and Weber, R., 2011. Semi-Supervised Constrained Clustering with Cluster Outlier Filtering. *In*: C. San Martin and S. Kim, eds. *Progress in Pattern Recognition, Image Analysis, Computer Vision, and Applications*. Heidelberg: Springer, 347–354.

Brunsdon, C., Fotheringham, S., and Charlton, M., 1998. Geographically Weighted Regression. *Journal of the Royal Statistical Society: Series D (The Statistician)*, 47 (3), 431–443.

Cadenasso, M., Pickett, S., and Schwarz, K., 2007. Spatial Heterogeneity in Urban Ecosystems: Reconceptualizing Land Cover and a Framework for Classification. *Frontiers in Ecology and the Environment*, 5 (2), 80–88.

Canli, E., Höfle, B., Hämmerle, M., Thiebes, B., and Glade, T., 2015. Permanent 3D Laser Scanning System for an Active Landslide in Gresten (Austria). *In*: *Geophysical Research Abstracts EGU General Assembly*. 2885.

Cochran, W., 1934. The Distribution of Quadratic Forms in a Normal System, with Applications to the Analysis of Covariance. *Mathematical Proceedings of the Cambridge Philosophical Society*, 30 (2), 178–191.

Csillag, F. and Sándor, K., 2002. Wavelets, Boundaries, and the Spatial Analysis of Landscape Pattern. *Écoscience*, 9 (2), 177–190.

Cuba, M., Leuangthong, O., and Ortiz, J., 2012. Detecting and Quantifying Sources of Non-Stationarity via Experimental Semivariogram Modeling. *Stochastic Environmental Research and Risk Assessment*, 26 (2), 247–260.

Cuzick, J. and Edwards, R., 1990. Spatial Clustering for Inhomogeneous Populations. *Journal of the Royal Statistical Society . Series B (Methodological)*, 52 (1), 73–104.

Darnieder, W., 2011. *Bayesian Methods for Data-Dependent Priors*. Columbus, OH: The Ohio State University.

Dray, S., 2011. A New Perspective about Moran's Coefficient: Spatial Autocorrelation as a Linear Regression Problem. *Geographical Analysis*, 43 (2), 127–141.

Dutilleul, P., 2011. *Spatio-Temporal Heterogeneity: Concepts and Analyses*. Cambridge, UK: Cambridge University Press.

Dutilleul, P. and Legendre, P., 1993. Spatial Heterogeneity Against Heteroscedasticity: An Ecological Paradigm Versus a Statistical Concept. *Oikos*, 66 (1), 152–171.

Fagan, W., Cantrell, R., and Cosner, C., 1999. How Habitat Edges Change Species Interactions. *The American Naturalist*, 153 (2), 165–182.

Fagan, W., Fortin, M., and Soykan, C., 2003. Integrating Edge Detection and Dynamic Modeling in Quantitative Analyses of Ecological Boundaries. *BioScience*, 53 (8), 730.

Fang, H. and Huang, D., 2004. Noise Reduction in LiDAR Signal Based on Discrete Wavelet Transform. *Optics Communications*, 233 (1–3), 67–76.

Fisher, P. and Robinson, V., 2014. Fuzzy Modelling. *In*: R. Abrahart and L. See, eds. *GeoComputation*. Boca Raton, FL: CRC Press, 283–306.

Forman, R., 1995. *Land Mosaics: The Ecology of Landscapes and Regions*. Cambridge, UK: Cambridge University Press.

Fortin, M., 1994. Edge Detection Algorithms for Two-Dimensional Ecological Data. *Ecology*, 75 (4), 956–965.

Fortin, M., 1999. Spatial Statistics in Landscape Ecology. *In*: J. Klopatek and R. Gardner, eds. *Landscape Ecological Analysis*. New York, NY: Springer, 253–279.

Fotheringham, A., Charlton, M., and Brunsdon, C., 1996. The Geography of Parameter Space: An Investigation of Spatial Non-Stationarity. *International Journal of Geographical Information Systems*, 10 (5), 605–627.

Fotheringham, A.S., Brunsdon, C., and Charlton, M., 2002. *Geographically weighted regression: the analysis of spatially varying relationships*. Chichester: John Wiley & Sons.

Gaetan, C. and Guyon, X., 2010. *Spatial statistics and modelling*. New York, NY: Springer.

Garrigues, S., Allard, D., Baret, F., and Weiss, M., 2006. Quantifying Spatial Heterogeneity at the Landscape Scale Using Variogram Models. *Remote Sensing of Environment*, 103 (1), 81–96.

Gelfand, A. and Banerjee, S., 2015. Bayesian Wombling: Finding Rapid Change in Spatial Maps. *Wiley Interdisciplinary Reviews: Computational Statistics*, 7 (October), 307–315.

Gelman, A., Carlin, J., Stern, H., Dunson, D., Vehtari, A., and Rubin, D., 2013. *Bayesian Data Analysis*. 3rd ed. Boca Raton, FL: CRC Press.

Getis, A., 2010. Spatial Autocorrelation. *In*: M. Fischer and A. Getis, eds. *Handbook of Applied Spatial Analysis*. Heidelberg: Springer, 255–278.

Getis, A., 2015. Analytically Derived Neighborhoods in a Rapidly Growing West African City: The Case of Accra, Ghana. *Habitat International*, 45 (Part 2), 126–134.

Getis, A. and Ord, J., 1992. The Analysis of Spatial Association by Use of Distance Statistics. *Geographical Analysis*, 24 (3), 189–206.

Godfrey, L., 1996. Some Results on the Glejser and Koenker Tests for Heteroskedasticity. *Journal of Econometrics*, 72 (1–2), 275–299.

Goovaerts, P., 2008. Accounting for Rate Instability and Spatial Patterns in the Boundary Aanalysis of Cancer Mortality Maps. *Environmental and Ecological Statistics*, 15 (4), 421–446.

Goovaerts, P., 2010. How do Multiple Testing Correction and Spatial Autocorrelation Affect Areal Boundary Analysis? *Spatial and Spatio-temporal Epidemiology*, 1 (4), 219–229.

Graif, C. and Sampson, R., 2009. Spatial Heterogeneity in the Effects of Immigration and Diversity on Neighborhood Homicide Rates. *Homicide Studies*, 13 (3), 242–260.

Grillet, M., Jordan, G., and Fortin, M., 2010. State Transition Detection in the Spatio-Temporal Incidence of Malaria. *Spatial and Spatio-temporal Epidemiology*, 1 (4), 251–259.

Hanson, T., Banerjee, S., Li, P., and McBean, A., 2015. Spatial Boundary Detection for Areal Counts. *In*: R. Mitra and P. Müller, eds. *Nonparametric Bayesian Inference in Biostatistics*. New York, NY: Springer, 377–399.

Höfle, B., Canli, E., Schmitz, E., Crommelinck, S., and Hoffmeister, D., 2016. 4D Near Real-Time Environmental Monitoring Using Highly Temporal LiDAR. *In*: *Geophysical Research Abstracts of the EGU General Assembly*.

Hope, A., 1968. A Simplified Monte Carlo Significance Test Procedure. *Journal of the Royal Statistical Society. Series B (Methodological)*, 30 (3), 582–598.

Hu, T., Liu, Q., Du, Y., Li, H., and Huang, H., 2015. Analysis of Land Surface Temperature Spatial Heterogeneity Using Variogram Model. *In*: *IEEE International Geoscience and Remote Sensing Symposium 2015*. Milan: IEEE, 132–135.

Hungr, O., Leroueil, S., and Picarelli, L., 2014. The Varnes Classification of Landslide Types, an Update. *Landslides*, 11 (2), 167–194.

Jaboyedoff, M., Oppikofer, T., Abellán, A., Derron, M., Loye, A., Metzger, R., and Pedrazzini, A., 2012. Use of LiDAR in Landslide Investigations: A Review. *Natural Hazards*, 61 (1), 5–28.

Jacquez, G., 2010. Geographic Boundary Analysis in Spatial and Spatio-Temporal Epidemiology: Perspective and Prospects. *Spatial and Spatio-Temporal Epidemiology*, 1 (4), 207–218.

Jacquez, G., Kaufmann, A., and Goovaerts, P., 2008. Boundaries, Links and Clusters: A New Paradigm in Spatial Analysis? *Environmental and Ecological Statistics*, 15 (4), 403–419.

Jacquez, G., Maruca, S., and Fortin, M., 2000. From Fields to Objects: A Review of Geographic Boundary Analysis. *Journal of Geographical Systems*, 2 (3), 221–241.

Jiang, B., 2015. Geospatial Analysis Requires a Different Way of Thinking: The Problem of Spatial Heterogeneity. *GeoJournal*, 80 (1), 1–13.

Keitt, T. and Urban, D., 2005. Scale-Specific Inference Using Wavelets. *Ecology*, 86 (9), 2497–2504.

Kent, M., Gill, W., Weaver, R., and Armitage, R., 1997. Landscape and Plant Community Boundaries in Biogeography. *Progress in Physical Geography*, 21 (3), 315–353.

Kent, M., Moyeed, R., Reid, C., Pakeman, R., and Weaver, R., 2006. Geostatistics, Spatial Rate of Change Analysis and Boundary Detection in Plant Ecology and Biogeography. *Progress in Physical Geography*, 30 (2), 201–231.

Koenker, R. and Bassett, G., 1982. Robust Tests for Heteroscedasticity Based on Regression Quantiles. *Econometrica*, 50 (1), 43–61.

Kolasa, J. and Rollo, C., 1991. The Heterogeneity of Heterogeneity: A Glossary. *In*: J. Kolasa and S. Pickett, eds. *Ecological Heterogeneity*. Heidelberg: Springer, 1–23.

Lague, D., Brodu, N., and Leroux, J., 2013. Accurate 3D Comparison of Complex Topography with Terrestrial Laser Scanner: Application to the Rangitikei Canyon (N-Z). *ISPRS Journal of Photogrammetry and Remote Sensing*, 82, 10–26.

Laurance, W., Didham, R., and Power, M., 2001. Ecological Boundaries: A Search for Synthesis. *Trends in Ecology & Evolution*, 16 (2), 70–71.

Lee, D. and Mitchell, R., 2012. Boundary Detection in Disease Mapping Studies. *Biostatistics*, 13 (3), 415–426.

Legewie, J. and Schaeffer, M., 2016. Contested Boundaries: Explaining Where Ethno-Racial Diversity Provokes Neighborhood Conflict. *American Journal of Sociology*, 122 (1), 125–161.

Lillesand, T., Kiefer, R., and Chipman, J., 2015. *Remote Sensing and Image Interpretation*. 7th ed. Hoboken, NJ: Wiley & Sons.

Lohrer, A., Rodil, I., Townsend, M., Chiaroni, L., Hewitt, J., and Thrush, S., 2013. Biogenic Habitat Transitions Influence Facilitation in a Marine Soft-Sediment Ecosystem. *Ecology*, 94 (1), 136–145.

Lovelace, R., Birkin, M., Cross, P., and Clarke, M., 2016. From Big Noise to Big Data: Toward the Verification of Large Data Sets for Understanding Regional Retail Flows. *Geographical Analysis*, 48 (1), 59–81.

Mandelbrot, B. and Hudson, R., 2004. *The (Mis)behavior of Markets: A Fractal View of Risk, Ruin, and Reward*. New York, NY: Basic Books.

Ord, J. and Getis, A., 1995. Local Spatial Autocorrelation Statistics: Distributional Issues and an Application. *Geographical Analysis*, 27 (4), 286–306.

Ord, J. and Getis, A., 2012. Local Spatial Heteroscedasticity (LOSH). *The Annals of Regional Science*, 48 (2), 529–539.

Ord, J.K. and Getis, A., 2001. Testing for local spatial autocorrelation in the presence of global autocorrelation. *Journal of Regional Science*, 41 (3), 411–432.

Páez, A. and Scott, D.M., 2004. Spatial statistics for urban analysis : A review of techniques with examples. *GeoJournal*, 61, 53–67.

Patil, G., Modarres, R., Myers, W., and Patankar, P., 2006. Spatially Constrained Clustering and Upper Level Set Scan Hotspot Detection in Surveillance Geoinformatics. *Environmental and Ecological Statistics*, 13 (4), 365–377.

Perkins, T., Scott, T., Le Menach, A., and Smith, D., 2013. Heterogeneity, Mixing, and the Spatial Scales of Mosquito-Borne Pathogen Transmission. *PLOS Computational Biology*, 9 (12), e1003327.

Sengstock, C., Gertz, M., Flatow, F., and Abdelhaq, H., 2013. A Probablistic Model for Spatio-Temporal Signal Extraction from Social Media. *In*: C. Knoblock and M. Schneider, eds. *Proceedings of the 21st ACM SIGSPATIAL International*

Conference on Advances in Geographic Information Systems (SIGSPATIAL'13). Orlando, FL: ACM, 264–273.

Sparrow, A., 1999. A Heterogeneity of Heteogeneities. *Trends in Ecology & Evolution*, 14 (11), 422–423.

Steiger, E., Resch, B., and Zipf, A., 2016. Exploration of spatiotemporal and semantic clusters of Twitter data using unsupervised neural networks. *International Journal of Geographical Information Science*, 30 (9), 1694–1716.

Strayer, D., Power, M., Fagan, W., Pickett, S., and Belnap, J., 2003. A Classification of Ecological Boundaries. *BioScience*, 53 (8), 723–729.

Tian, P., Cao, X., Liang, J., Zhang, L., Yi, N., Wang, L., and Cheng, X., 2014. Improved Empirical Mode Decomposition Based Denoising Method for LiDAR Signals. *Optics Communications*, 325, 54–59.

Tukey, J., 1977. *Exploratory Data Analysis*. Boston, MA: Addison-Wesley.

Turner, M., 1989. Landscape Ecology: the Effect of Pattern on Process. *Annual Review of Ecology and Systematics*, 20 (1), 171–197.

Wagner, H. and Fortin, M., 2005. Spatial Analysis of Landscapes: Concepts and Statistics. *Ecology*, 86 (8), 1975–1987.

Walck, C., 2007. *Hand-Book on Statistical Distributions for Experimentalists*. Stockholm: University of Stockholm.

Wang, J., Zhang, T., and Fu, B., 2016. A Measure of Spatial Stratified Heterogeneity. *Ecological Indicators*, 67, 250–256.

Womble, W., 1951. Differential Systematics. *Science*, 114 (2961), 315–322.

Xu, M., Mei, C., and Yan, N., 2014. A Note on the Null Distribution of the Local Spatial Heteroscedasticity (LOSH) Statistic. *The Annals of Regional Science*, 52 (3), 697–710.

Ye, X., Wang, T., Skidmore, A., Fortin, D., Bastille-Rousseau, G., and Parrott, L., 2015. A Wavelet-Based Approach to Evaluate the Roles of Structural and Functional Landscape Heterogeneity in Animal Space Use at Multiple Scales. *Ecography*, 38 (7), 740–750.

Appendix A: Relationship between LOSH and LSD

The ratio between LOSH and LSD is given by

$$\frac{H_i}{LSD_i} = \frac{\frac{1}{n_i}\sum_{j\in\mathcal{N}_i}\left|e_j\right|^2 \cdot \sum_{j\in\mathcal{N}} w_{ij}\left|e_j\right|^2 \cdot \sum_{j\in\mathcal{N}} w_{ij}}{\frac{1}{n}\sum_{j\in\mathcal{N}}\left|e_j\right|^2 \cdot \sum_{j\in\mathcal{N}} w_{ij}\left|e_j\right|^2 \cdot \sum_{j\in\mathcal{N}} w_{ij}} = \frac{n \cdot h_i}{\sum_{j\in\mathcal{N}}\left|e_j\right|^2} = h_i \cdot h_1^{-1}.$$

From this, LOSH and LSD can be inferred:

$$H_i = \frac{LSD_i \cdot h_i}{h_1} \quad \text{and} \quad LSD_i = \frac{H_i \cdot h_1}{h_i}.$$

The ratio above shows that LSD can be turned into LOSH and vice versa, demonstrating that both measures represent a scaled version of the respective other.

Appendix B: Expectation and variance of spatially weighted mean estimates

The mean and the variance of the spatially weighted mean estimates Y_j are affected by the spatial weighting structure. Let $\{X_k\}$ be independent real random variables indexed over the neighbourhood set of spatial units $\mathcal{N}_j$. Let further $\{w_{jk}\}$ denote the set of spatial weights upon $\mathcal{N}_j$ that sums up to $W_j = \sum_{k\in\mathcal{N}_j} w_{jk}$, and $Y_j = \left(1/W_j\right)\sum_{k\in\mathcal{N}_j} w_{jk}x_k$ be a local spatial average as defined in Equation (1). Under local randomisation the expectation $E[Y_j]$ is given by

$$E\left[\frac{1}{W_j}\sum_{k\in\mathcal{N}_j} w_{jk}X_k\right] = \frac{1}{W_j}\sum_{k\in\mathcal{N}_j} w_{jk}E[X_k] = \frac{1}{W_j}\sum_{k\in\mathcal{N}_j} w_{jk}\mu_{X_j} = \mu_{X_j}.$$

The location of the mean is thus not affected by the spatial weights. Note that the weighted sample mean is a linear combination $\left(w_{j1}/W_j\right)X_1 + \cdots + \left(w_{jn_j}/W_j\right)X_{n_j}$ of independent random variables (i.e., local independent under the randomisation assumption of H_0 *of LSD*). The variance of Y_j is therefore obtained by applying the rule for the variance of linear combinations of independent random variables, which is given by $Var[\sum_k a_k X_k] = \sum_k a_k^2 Var[X_k]$, and thus for Y_j yields

$$Var[Y_j] = \sum_{k\in\mathcal{N}_j}\left(\frac{w_{jk}}{W_j}\right)^2\sigma^2_{\mathcal{N}_j} = \sigma^2_{\mathcal{N}_j}\cdot\sum_{k\in\mathcal{N}_j}\frac{w_{jk}^2}{W_j^2}.$$

Unlike the mean value, the variance is scaled by the weighting scheme. The above relationship for the variance is demonstrated for the ordinary unweighted case through substituting *1* for each weight w_{jk}. Their sum then yields n_j and the above equation reduces to the variance of the unweighted sample mean $\sigma^2_{\mathcal{N}_j}\sum_{k=1}^{n_j}\left(1^2/n_j^2\right) = \sigma^2_{\mathcal{N}_j}/n_j$.

Appendix C: Averaging of several local variances

The variance of a random variable X is generally given by the shift rule $Var[X] = E[X^2] - E[X]^2$. We already determined the estimator of $E[X]^2$ in Equation (8), which is $\bar{x}_c^2$. The estimator of $E[X^2]$ takes the form $\sum_{i=1}^n x_i^2/n$, though it must take into account the grouping in the data (i.e., the spatially overlapping neighbourhoods). To simplify the following steps, the Bessel correction of the unbiased sample variance s^2_{n-1} is reversed first:

$$\dot{s}^2 = \left(\frac{n-1}{n}\right)s^2_{n-1} = \frac{1}{n}\sum\nolimits_{i=1}^{n}(x_i - \bar{x})^2 = \left(\frac{1}{n}\sum\nolimits_{i=1}^{n}x_i^2\right) - \bar{x}^2.$$

From this, the corresponding sum of squares is obtained:

$$n(\dot{s}^2 + \bar{x}^2) = \sum\nolimits_{i=1}^{n}x_i^2.$$

This sum of squares can be split up into a series of partial sums. For the case of partly overlapping spatial neighbourhoods this gives $\sum_{i\in\mathcal{N}_1}x_i^2 + \cdots + \sum_{i\in\mathcal{N}_n}x_i^2$. Each of these

summations can be represented through their respective local sample variance and local mean value. We get that

$$\sum_{i\in\mathcal{A}_i}\sum_{j\in\mathcal{N}_i} x_j^2 = \sum_{i\in\mathcal{A}_i} n_i(\dot{s}_i^2 + \bar{x}_i^2),$$

and the substitution of this back into $Var[X] = E[X^2] - E[X]^2$ yields

$$\dot{s}_c^2 = \frac{\sum_{j\in\mathcal{A}_i} n_j\left(\dot{s}_j^2 + \bar{x}_j^2\right)}{\sum_{j\in\mathcal{A}_i} n_j} - \bar{x}_c^2.$$

In order to obtain an unbiased result, we reverse the previous elimination of the Bessel correction. The rescaled version of $\dot{s}_c^2$ is

$$s_c^2 = \frac{\sum_{j\in\mathcal{A}_i} n_j}{\left(\sum_{j\in\mathcal{A}_i} n_j\right) - n_{\mathcal{A}_i}} \cdot \dot{s}_c^2 = \frac{\sum_{j\in\mathcal{A}_i}\left(n_j - 1\right)\left(s_j^2 + \bar{x}_j^2\right)}{\left(\sum_{j\in\mathcal{A}_i} n_j\right) - n_{\mathcal{A}_i}} - \bar{x}_c^2.$$

Appendix D: Derivation of the prior

The prior combines the two marginal densities

$$f\left(\mu_{X_j} \mid \sigma_{X_j}^2; \mu_0, \sigma_0^2 = \sigma_{X_j}^2/n_i\right) = \frac{\sqrt{n_i}}{\sqrt{2\pi}\sigma_{X_j}} \exp\left(-\frac{n_i\left(\mu_{X_j} - \mu_0\right)^2}{2\sigma_{X_j}^2}\right)$$

and

$$f\left(\sigma_{X_j}^2; \upsilon_0, \tau_0^2\right) = \frac{\left(\frac{\tau_0^2\upsilon_0}{2}\right)^{\upsilon_0/2}}{\Gamma\left(\frac{\upsilon_0}{2}\right)\sigma_{X_j}^{2+\upsilon_0}} \exp\left(-\frac{\upsilon_0\tau_0^2}{2\sigma_{X_j}^2}\right)$$

into their joint product

$$\pi\left(\mu_{X_j}, \sigma_{X_j}^2\right) = \frac{\left(\frac{\tau_0^2\upsilon_0}{2}\right)^{\upsilon_0/2}}{\sqrt{2\pi}\sigma_{X_j}\sqrt{n_i}\cdot\Gamma\left(\frac{\upsilon_0}{2}\right)\sigma_{X_j}^{2+\upsilon_0}} \cdot \exp\left(-\frac{n_i\left(\mu_{X_j} - \mu_0\right)^2 + \upsilon_0\tau_0^2}{2\sigma_{X_j}^2}\right),$$

where Γ is the gamma function. If all normalising constants are omitted, the prior is obtained as follows:

$$\pi\left(\mu_{X_j}, \sigma_{X_j}^2\right) \propto \frac{1}{\sigma_{X_j}^{3+\upsilon_0}} \cdot \exp\left(-\frac{n_i\left(\mu_{X_j} - \mu_0\right)^2 + \upsilon_0\tau_0^2}{2\sigma_{X_j}^2}\right).$$

Appendix E: Derivation of the posterior

The observed data $Y_i \sim N\left(\mu_{X_i}, \sigma_{X_i}^2\right)$ is described by the normal likelihood function

$$f\left(Y_i \mid \mu_{X_i}, \sigma_{X_i}^2\right) = \frac{1}{\sqrt{2\pi}\,\sigma_{X_i}} \cdot \exp\left(-\frac{\left(Y_i - \mu_{X_i}\right)^2}{2\sigma_{X_i}^2}\right) \propto \sigma^{-1} \cdot \exp\left(-\frac{\left(Y_i - \mu_{X_i}\right)^2}{2\sigma_{X_i}^2}\right).$$

The multiplication of this likelihood by the prior from Appendix D yields the following posterior density:

$$f\left(\mu_{X_i}, \sigma_{X_i}^2 \mid Y_i\right) \propto \frac{\left(\frac{\tau_0^2 \upsilon_0}{2}\right)^{\upsilon_0/2}}{2\pi\sqrt{n_i} \cdot \Gamma\left(\frac{\upsilon_0}{2}\right) \sigma_{X_i}^{4+\upsilon_0}} \cdot \exp\left(-\frac{n_i\left(\mu_{X_i} - \mu_0\right)^2 + \left(Y_i - \mu_{X_i}\right)^2 + \upsilon_0\tau_0^2}{2\sigma_{X_i}^2}\right).$$

After again omitting all normalising constants, we arrive at

$$f\left(\mu_{X_i}, \sigma_{X_i}^2 \mid Y_i\right) \propto \frac{1}{\sigma_{X_i}^{4+\upsilon_0}} \cdot \exp\left(-\frac{n_i\left(\mu_{X_i} - \mu_0\right)^2 + \left(Y_i - \mu_{X_i}\right)^2 + \upsilon_0\tau_0^2}{2\sigma_{X_i}^2}\right),$$

which is the non-normalised posterior density.